Aeolian Research xxx (2011) xxx–xxx

Contents lists available at ScienceDirect

Aeolian Research

journal homepage: www.elsevier.com/locate/aeolia

Review Article

Temperate grasslands as a dust source: Knowledge, uncertainties, and challenges

M. Shinoda [a,*], J.A. Gillies [b], M. Mikami [c], Y. Shao [d]

[a] Arid Land Research Center, Tottori University, 1390 Hamasaka, Tottori 680-0001, Japan
[b] Division of Atmospheric Sciences, Desert Research Institute, 2215 Raggio Parkway, Reno, NV 89512, USA
[c] Meteorological Research Institute, Nagamine 1-1, Tsukuba, Ibaraki 305-0052, Japan
[d] Institute of Geophysics and Meteorology, University of Cologne, Cologne, Germany

ARTICLE INFO

Article history:
Received 16 March 2011
Accepted 6 July 2011
Available online xxxx

Keywords:
Wind erosion
Dust emission
Dust storm
Vegetation effect
Land degradation

ABSTRACT

Temperate grasslands are sensitive to climate change and are significant, or potentially significant, dust sources. Temperate grassland aeolian processes are unique in that the vegetation growth-decay cycle and weathering process due to extreme temperature changes profoundly affect the occurrence and intensity of wind erosion and dust emission. Human activities, such as animal husbandry or cultivation, also may result in land degradation and enhanced wind erosion. So far, little systematic research on temperate grassland wind erosion has been done, but this issue deserves particular attention. In this review paper, we summarize the understanding of temperate grassland wind-erosion processes and identify the uncertainties and research needs. The needs include (1) a deeper understanding of the aerodynamic and physical controls of grassland vegetation on wind erosion and dust emission processes, (2) scaling known relationships upwards to model the regional scale, (3) quantifying critical parameters affecting dust emissions (i.e., surface and aerodynamic roughness) via remote-sensing techniques, and (4) integrated wind-erosion modeling that incorporates grassland aeolian database and vegetation modeling of both seasonal growth and decay plus the impacts of grazing and cultivation. We also outline the research being carried out by Japanese scientists in collaboration with colleagues at Mongolian, American, and German research institutes in developing a temperate grassland wind-erosion modeling system, which can be used as a pre-warning system of severe dust storms and as a tool for strategic management of temperate grasslands.

Contents

1. Introduction . . . 00
2. Grasslands wind erosion and dust patterns . . . 00
3. Vegetation and aeolian processes . . . 00
4. Modeling of dust emissions with applications to TGs . . . 00
   4.1. WEQ and WEPS . . . 00
   4.2. Integrated wind-erosion models . . . 00
   4.3. Vegetation modeling . . . 00
   4.4. Future grassland wind-erosion modeling system . . . 00
      4.4.1. Vegetation growth and decay . . . 00
      4.4.2. Model and data assimilation (with a focus on soil moisture and vegetation) . . . 00
      4.4.3. Supply limited wind erosion . . . 00
      4.4.4. Establishment of grassland aeolian database . . . 00
5. Monitoring . . . 00
   5.1. Requirements for dust monitoring over TGs . . . 00
      5.1.1. Monitoring parameters . . . 00
      5.1.2. Monitoring of sand and dust fluxes . . . 00
   5.2. Monitoring of the processes over Northeastern Asia . . . 00
   5.3. Monitoring needs . . . 00

* Corresponding author. Tel./fax: +81 857 21 7030.
E-mail addresses: shinoda@alrc.tottori-u.ac.jp (M. Shinoda), jackg@dri.edu (J.A. Gillies), mmikami@mrima.go.jp (M. Mikami), yshao@meteo.Uni-Koeln.DE (Y. Shao).

1875-9637/$ - see front matter © 2011 Published by Elsevier B.V.
doi:10.1016/j.aeolia.2011.07.001

6. Concluding remarks 00
Acknowledgements 00
References 00

1. Introduction

Temperate grasslands (TGs) are situated in mid-latitude regions where climatic conditions favor the dominance of perennial grasses (Archibold, 1995). The most extensive TGs are the prairies of North America, which used to cover 350 million ha but now cover about 60 million ha. In Eurasia, steppes cover 250 million ha of rolling plains extending from Hungary to Northeast China (Fig. 1; Eurasian grasslands are referred hereafter as steppes). In the Southern Hemisphere, TGs are represented by the pampas of Argentina and the veld of high plateaus of southern Africa. TGs form a buffer zone between deserts and forests and can act as a frontier for expansion of deserts or forests depending on prevailing climatic conditions. The steppes east of the Ural Mountains, highlighted in the present paper, have an annual precipitation ranging from 400 mm in the north to 200 mm in the south (Archibold, 1995).

TGs deserve particular attention from aeolian researchers because they are subject to severe seasonal wind erosion activities that threaten sustainability of the TG ecosystem. Sustainability of this grassland ecosystem critically depends on interactions between climate change, grassland vegetation, and human activities. Aeolian processes play a major role in these interactions. For example, overgrazing may result in decreased vegetation and enhanced wind erosion that restricts recovery of grasslands in the subsequent growing season. Continued overgrazing and wind erosion prevent recovery of grasses. Moreover, a marked drying trend in the arid region of eastern Eurasia during the past century (IPCC WG 1, 2007) may have had an adverse impact roughly equivalent to that of overgrazing. It may be expected that TGs, given their sensitivities to climate change and increased anthropogenic pressures (e.g., overgrazing), could become an even more significant contributor to the global dust cycle. With the pressing need for aeolian research on grasslands, a wide range of specific issues arise as described below.

Severe dust storms pose a serious threat to grassland livestock and sometimes human lives. For example, 120,000 and 110,000 animals were killed in China during the 5 May 1993 and 14–16 April 1998 dust storms, respectively (Shao and Dong, 2006). A severe storm with dust and snow in eastern Mongolia on 26–27 May 2008 resulted in record-level damages, killing 52 people and 280,000 animals (Chimgee et al., 2010). The need for developing an early warning system to ameliorate damages is apparent.

TG wind-erosion events often are severe and cause marked deformations to the landscape and damage to plants. Saltating sand grains cause damage to the epidermis of leaves, increasing plant wilting and mortality (Mainguet, 1999). In extreme cases, plants can be buried by sand drifts from which they cannot recover. In eroded areas, the soil water-holding capacity is reduced; plants are uprooted; and fertile top soils that contain organic matter, nutrients, and almost all seeds are irreversibly removed (Zobeck and Fryrear, 1986). The positive feedback between wind erosion and reduction of vegetative health must be checked to prevent grassland degradation.

The combined areas of the northeast Asian deserts located in Mongolia and China (>1.6 million km^2, Mildred, 1984; Zhu et al., 1980) make this region the second largest dust source on the planet (Tanaka and Chiba, 2005). Dust from this region has been found in Greenland and throughout the Arctic, because Mongolia and China are the northern most arid source areas and their high altitude facilitates long-distance dust transport by westerly winds (Svensson et al., 2000). Under the continued pressure of global climate change and human interferences, TGs may become of greater importance in the global dust cycle. This has ramifications for the global radiation budget (Sokolik et al., 2001), cloud processes (Sassen et al., 2003; Li et al., 2010), air pollution (Husar et al., 2001), and redistribution of carbon and iron on the global scale (Mahowald et al., 2010). Therefore, study of grassland aeolian processes is indispensible to global climate and dust cycle research.

The dynamics of wind erosion in TGs have unique features (Fig. 2). Most noticeably, the vegetation growth-decay cycle plays a major role in seasonal variations of wind-erosion activities. For example, Mongolian grasslands experience severe wind erosion in spring probably due to the lack of aboveground phytomass

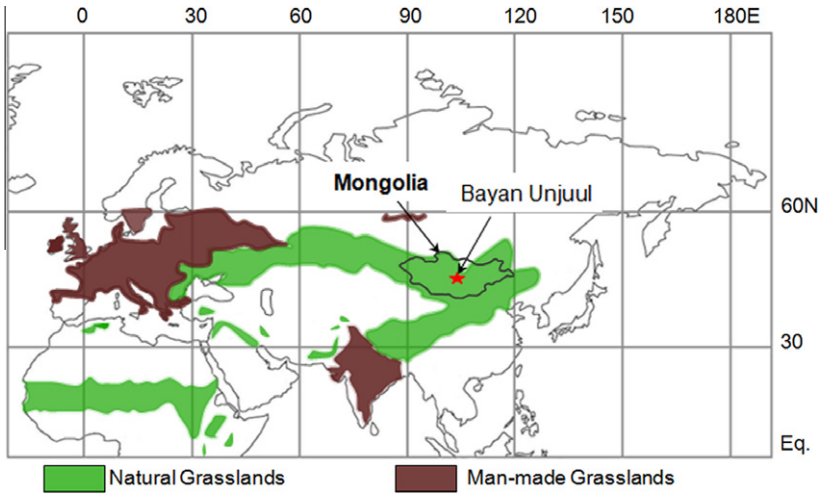

Fig. 1. Grasslands in Eurasia and Africa modified from Wiegand et al. (2008a), and the study site of the Dust-Vegetation Interaction Experiment (DUVEX) project (Bayan Unjuul, star).

Please cite this article in press as: Shinoda, M., et al. Temperate grasslands as a dust source: Knowledge, uncertainties, and challenges. Aeolian Research (2011), doi:10.1016/j.aeolia.2011.07.001

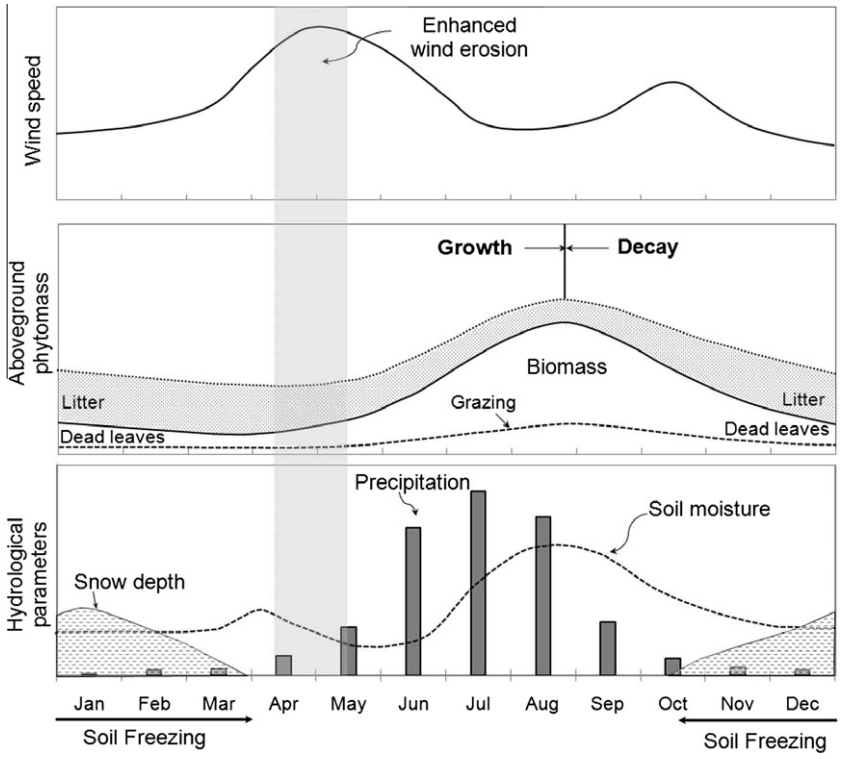

Fig. 2. Typical seasonal changes of wind speed, aboveground phytomass, and hydrological parameters in the Mongolian steppe and their relationships with wind erosion. The horizontal arrow denotes the period of soil freezing. Phytomass equals to biomass (living materials) plus dead leaves.

(Shinoda et al., 2010a) and occurrence of strong winds (Kurosaki and Mikami, 2005). In the growing season, however, wind erosion is almost negligible. Aerodynamic characteristics and the protective effects of vegetation substantially differ during the seasons of growth and decay. TGs experience large amplitudes of seasonal change in temperature across the freezing point. These changes promote soil weathering processes particularly by freeze–thaw mechanisms, unlike lower latitude dust source areas.

While much research has been done on wind erosion and dust emissions in warm deserts areas (e.g., Nickling and Gillies, 1989, 1993; Marticorena and Bergametti, 1996; Washington and Todd, 2005) and agricultural systems (e.g., Gillette, 1988; Zobeck, 1991; Hagen, 1991; Stout and Zobeck, 1996), relatively few studies (but see Hoffmann et al., 2008a) are dedicated to TGs with their characteristic grass communities and higher latitude climate conditions. From a modeling perspective, dust assessment and prediction systems that integrate atmospheric, land-surface, and wind-erosion models with GIS database and observations have been developed for TGs (e.g., Shao and Dong, 2006). Although effort has been made to develop a suitable database for land-surface parameters (e.g., soil texture, fraction of cover, and aerodynamic roughness), growth and decay of grassland vegetation have not been included in existing wind-erosion models. From a monitoring perspective, new instruments for measuring sand drift and dust emissions have been developed (e.g., Mikami et al., 2005; Etyemezian et al., 2007). These instruments have been used successfully to study bare-soil wind-erosion processes but have been less utilized in TG environments. Because wind erosion in grasslands depends on vegetation cover (Kimura et al., 2009; Kimura and Shinoda, 2010), soil moisture (Ishizuka et al., 2005; Kimura et al., 2009), and snow cover (Kurosaki and Mikami, 2004), field measurements are necessary to better understand TG wind erosion processes.

In this review paper, we summarize the understanding of TG wind-erosion processes and identify critical areas of research needs. We begin by describing the roles of TGs in the global ecosystem and dust cycle. This is followed by sections on grassland wind erosion dynamics and the modeling and monitoring of TG wind-erosion processes.

We also introduce research being carried out by Japanese scientists in collaboration with colleagues at Mongolian, American and German research institutions to illustrate components of the TG aeolian system and efforts underway in developing a TG wind-erosion modeling and prediction system. This modeling system is being developed to provide early warnings of severe dust storms, and will serve as a tool for strategic management of TG ecosystems.

2. Grasslands wind erosion and dust patterns

The arid and semiarid areas in Mongolia and China consist of the Gobi and Taklimakan deserts, as well as surrounding grasslands. The Gobi and Taklimakan deserts cover approximately 1,295,000 (Mildred, 1984) and 337,600 (Zhu et al., 1980) km^2 (in total, 1,632,600 km^2), respectively. The Sahara desert, Earth's largest dust source area by comparison, is 7,000,000 km^2 (Cooke et al., 1993). The dust climatology of TGs in northeast Asia is now fairly well understood based on analyses of weather records during the past 50 years (Chun et al., 2001; Qian et al., 2002; Kurosaki and Mikami, 2005; Shao and Dong, 2006) and recent satellite data (Prospero et al., 2002). These data consistently show that the Tarim Basin has a very high frequency of dust events, with the highest (47%) recorded at Hetian (80°E, 37°N). The Gobi is another region of frequent dust events, with the highest (15%) recorded along the China–Mongolia border. In Mongolia, the highest dust-storm frequency occurs at the southern side of the Altai Mountains, the Ulaan-nuur area and the Zamiin-Uud area (Natsagdorj et al., 2003). The highest mean annual number of dust-storm days of 34.4 is recorded at Zamiin-Uud (Middleton, 1991). The Great Lakes Depression to the northwest of Mongolia is another region of high dust frequency.

Please cite this article in press as: Shinoda, M., et al. Temperate grasslands as a dust source: Knowledge, uncertainties, and challenges. Aeolian Research (2011), doi:10.1016/j.aeolia.2011.07.001

There are two sets of controls on erosion by any process: the forces that can liberate particles from the main soil mass (*erosivity*) and susceptibility of a soil to loss of material (*erodibility*) (UNEP, 1997). Erosivity is controlled primarily by wind strength, while erodibility is linked to land-surface conditions. Soil erodibility in grasslands is complicated by winter snow and the growth cycle of vegetation. Fig. 3 shows climatological seasonal changes in dust-event frequencies, snow cover (retrieved from the Defense Meteorological Satellite Program (DMSP) Special Sensor Microwave/Imager (SSM/I), and vegetation cover (retrieved from the NOAA satellite) in East Asia (Kurosaki and Mikami, 2007). Kurosaki and Mikami (2007) observed for Mongolia that wind erosion is weak in January due to extensive snow cover, April is the peak dust month, in July the area is fully protected from wind erosion by vegetation, and by October the surface is still sufficiently well protected by residual grasses. Kimura and Shinoda (2010) demonstrated the correlation between the normalized difference vegetation index (NDVI) in the summer and that in the following spring, which shows that vegetation conditions have seasonal linkages. Zou and Zhai (2004) found that a lower vegetation cover in

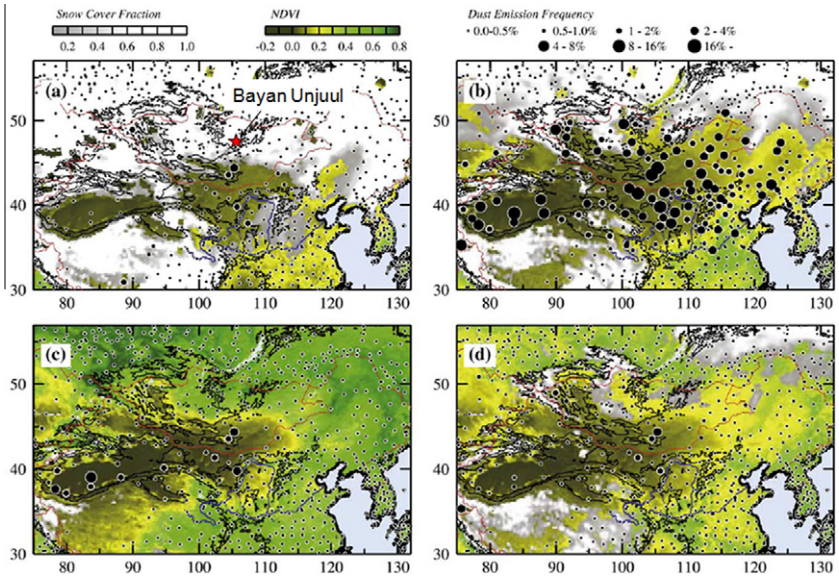

Fig. 3. Dust-event frequency, snow-cover fraction and NDVI (indicated respectively by solid circles, white–grey hatching and green–brown hatching) in East Asia for (a) January; (b) April; (c) July; and (d) October (modified from Kurosaki and Mikami, 2007). The star symbol in Fig. 3a indicates the study site for the DUVEX project (Bayan Unjuul).

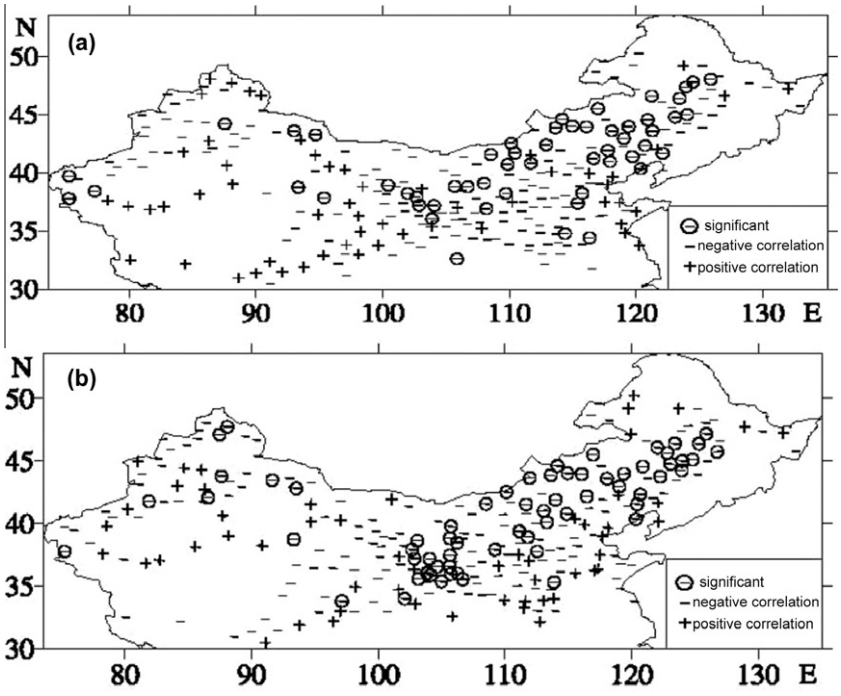

Fig. 4. (a) Correlation coefficients between NDVI and number of dust-storm days in the same spring over northern China (minus and plus signs represent negative and positive correlations, respectively; minus with circle signs represent significant negative correlations with values less than −0.44; and the calculation period is 1982–2001). (b) As (a), but correlation between summer NDVI and number of dust-storm days of the next spring (from Zou and Zhai, 2004).

Please cite this article in press as: Shinoda, M., et al. Temperate grasslands as a dust source: Knowledge, uncertainties, and challenges. Aeolian Research (2011), doi:10.1016/j.aeolia.2011.07.001

northern China in a particular year is correlated with a high frequency of dust storms in the spring of the following year (Fig. 4).

Freeze–thaw processes affect soil structure and weaken aggregate stability leading to increased erodibility (Bullock et al., 2001). These processes may be enhanced in TGs due to the presence of greater amounts of soil water than found in warm deserts; and the processes can effectively operate during the spring and autumn in some TGs, such as those in Mongolia, when temperatures fluctuate across the freezing point in the diurnal cycle.

Residuals of senescent leaves remain from the previous summer growing season in various amounts from year-to-year, affecting the amount of standing stubble and prostrate cover that offer protection to the surface. The winter conditions and remains of the previous year's vegetation create initial conditions that affect the aeolian transport system as it activates during the spring. In Mongolia, the dust season is confined to the periods when the surface is dry and free from snow and vegetation cover is at a minimum. Soil moisture is usually the lowest in the spring (Nandintsetseg and Shinoda, 2010), as evaporation is high due to strong winds and snowmelt is reduced due to a limited snow pack (Morinaga et al., 2003).

Surface soil moisture critically affects the threshold velocity of wind erosion (e.g., Sherman, 1990; Fécan et al., 1999). Nandintsetseg and Shinoda (2010) studied the spatial pattern of soil moisture in Mongolia and found that there is a general trend of decreasing soil moisture from the north to south.

As for soil erosivity, seasonal variations in grassland wind-erosion activities are strongly influenced by wind speed. Strong winds occur most frequently in spring and least frequently in winter and summer (Kurosaki and Mikami, 2005). A weak secondary frequency peak of strong wind occurs around October; and dust can be generated, but the dust-event frequency has no obvious peak at this time. The synoptic systems that generate severe dust storms are mostly cold air outbreaks associated with intense low-pressure systems. The eastward and south-eastward moving cyclones and strong post-frontal northwesterly wind (mostly between 8 and 18 m s^{-1}) can transport large amounts of dust to the eastern parts of China, Korea, and Japan (Shao and Wang, 2003). As mentioned earlier, dust originating from northeast Asia is the main contributor to the dust found in Greenland and throughout the Arctic.

There are two seasons of enhanced wind erosion as a consequence of a combination of vegetation cover, snow cover, and wind speed. In winter, soil is covered by snow or is frozen and winds are weak, thus the soil is protected from erosion. In summer, soil is protected from erosion by increased vegetation cover due to increased precipitation under conditions of weaker winds. The main erosion season occurs in March, April, and May when most severe dust storms occur. A second season exists around October, but dust activities are much reduced by comparison.

Grasslands are likely subjected to grazing pressure all year round, which affects soil erodibility. This pressure has increased in recent years (Sugita et al., 2007). Wind erosion on disturbed soil surfaces is typically an order of magnitude greater than on undisturbed soil surfaces because freshly exposed soils contain more erodible particles than natural soils (Macpherson et al., 2008). Mechanical disturbance of the soil by grazing animals can break physical bonds between particles with a loss of cohesive strength, which increases the likelihood for transport threshold to be reached at lower wind speeds (Belnap and Gillette, 1997). Experiments with portable wind tunnels (e.g., Gillette et al., 1980; Nickling and Gillies, 1989; Macpherson et al., 2008) have shown that threshold velocity increases with different types of desert soil surfaces in the following order: disturbed soils, sand dunes, alluvial and aeolian sand deposits, disturbed playa soils, skirts of playas, playa centers, and desert pavements. Other wind-tunnel studies have demonstrated that erosion can be accelerated by a factor of 10 by cultivation, 1.14 by overgrazing, and 22.8 by overcutting (Shi et al., 2004).

Overcultivation, overgrazing and overharvesting on grasslands lead to their degradation. A global assessment of land degradation indicates that the grassland area in northeast China is a hot spot of wind and water erosion due to decreased vegetation cover (Lepers et al., 2005). The most recent assessment for Mongolia suggests 78.2% of the territory has been affected by moderate to very severe desertification (mainly in terms of soil erosion) due to overgrazing (Mandakh et al., 2007).

Soils in TGs account for about 6% of terrestrial soils but store about 15% of total soil carbon. Grassland wind erosion can cause a considerable loss of soil organic carbon and nutrients (Hoffmann et al., 2008a,b), which is strengthened especially over cultivated land surface (e.g. Gregorich et al., 1998; Wang et al., 2006). In areas with annual precipitation less than 300 mm, sediment transport due to wind erosion is generally greater than that due to water erosion (Cooke et al., 1993). The annual precipitation in TGs varies in the range across this critical value (Archibold, 1995). In these regions, wind and water erosion operate interactively and complementarily, but with different spatial and temporal intensities (Cooke et al., 1993). For example, surface sediments are transported by fluvial processes and deposited downstream in lowlands such as wadis or playas primarily during the summer rainy season. During the dry season, dusts are entrained by wind from the ground and transported in suspension, while sand-sized grains move downwind in saltation or creep. The redistribution of carbon within the grassland geo-ecosystem and the contribution of grassland wind and water erosion to the global carbon balance deserve much more thorough investigations. So far, modeling and observational efforts mostly have been concerned with carbon redistribution due to water erosion (e.g., Van Oost et al., 2007).

There is considerable spatial heterogeneity within the grassland system with respect to dust cycling. Grassland soils sometimes act as dust sources, but also frequently benefit from dust deposition (Hoffmann et al., 2008a,b; Liu et al., 2008). The rates of dust emission and deposition vary profoundly over space and through time and it remains to be determined what areas within them are net dust sources or sinks. It is, however, reasonable to believe that grassland wind erosion results in net soil organic carbon export, because dust deposited to the region is often desert dust from upwind sources with low carbon content, while dust emitted from a TG region is typically rich in organic carbon.

3. Vegetation and aeolian processes

In arid lands with predominantly shrub vegetation, sand movement drops sharply as shrub cover thickens from 15% to 25% (Wasson and Nanninga, 1986). As for short grasses that dominate in the TGs, the threshold of vegetation cover above which wind erosion is efficiently eliminated is 15–20% (Buckerly, 1987; Lancaster and Baas, 1998; Kimura et al., 2009). Grasses, however, have a complex morphological and drag coefficient response to winds, which depends on their flexibility. Gillies et al. (2000, 2006, 2010) have shown that the threshold for sand transport, the magnitude of sand transport, and the degree of protection provided by roughness elements to the surface all depend on plant morphology, geometry, and wind speed. Changes in grassland morphology and geometry can cause seasonal and interannual fluctuations of threshold wind speed for wind erosion (Fig. 2). In addition to natural variations, grassland vegetation also is subject to changes induced by grazing, fire, and cultivation (Archibold, 1995), which in turn affect the processes of wind erosion. Human introduced (as well as water-erosion induced) disturbances to grassland surfaces generally make the soils more erodible by wind in two ways: (a) by loosening

Please cite this article in press as: Shinoda, M., et al. Temperate grasslands as a dust source: Knowledge, uncertainties, and challenges. Aeolian Research (2011), doi:10.1016/j.aeolia.2011.07.001

inter-particle bonds (Cooke et al., 1993) and (b) by reduced vegetation affecting the transfer of momentum in the atmospheric surface layer and localized patterns of turbulence.

At critical levels of vegetation cover, arid land systems such as those of the TGs can become vulnerable to wind erosion processes. In TGs vegetation is predominantly grass that cycles through a growth pattern, which at different times of the year can include live plants, senescent plants, and mixtures of standing and prostrate plants (or plant parts) that create different amounts of protection for the soil. The standing and prone, living, or residual vegetation protects the surface differently and with different efficiencies. Based on research by Lyles and Allison (1976), Hagen et al. (1996a,b) and Bilbro and Fryrear (1994), standing vegetation is approximately five times more effective per unit area in reducing surface shear stress than cover per unit area. Li et al. (2007) reported that as the lateral cover (LC) of grass-type vegetation, defined as $N \times A_p$ (where N is the number density of plants and A_p is the total area of plants projected onto a plane perpendicular to the ground and the direction of wind divided by the ground area in which the plants were measured [Okin, 2005]), decreased below approximately 9%, wind erosion and dust flux increased dramatically from their test surfaces in the Chihuahuan Desert near Las Cruces, New Mexico.

The shear stress generated by wind flowing over the surface becomes partitioned in a sparsely vegetated community between the plants that protrude into the boundary layer and the open ground between them. Schlichting (1936) first described the partitioning of shear stress between roughness elements and a smoother intervening surface. This approach is inherently applicable to understanding the aerodynamics of a sparse vegetative canopy and its effect on wind erosion and dust emissions. Shear stress partitioning has been used to evaluate the role that roughness elements exert on the threshold of entrainment of particles in the presence of solid element roughness (e.g., Gillette and Stockton, 1989; Musick, 1999; Nickling and McKenna Neuman, 1995; Gillies et al., 2007) and its effects on sediment transport rates (e.g., Orndorff, 1998; Gillies et al., 2006) as well as the evaluation of how vegetation decreases wind erosion in rangelands (Stockton and Gillette, 1990; Wolfe and Nickling, 1996).

Raupach et al. (1993) presented a model that evaluates the partitioning of wind shear stress between non-erodible roughness elements and the bare intervening surface. This relationship is expressed in terms of the threshold friction velocity (or wind shear velocity) ratio (R_t), which defines the ratio between the threshold friction velocity over a smooth surface and a similar surface covered with non-erodible roughness elements. The friction velocity (u_*, m s^{-1}) describes the magnitude of shear stress imparted by the wind on the surface as defined by the "law of the wall" represented by the equation:

$$\frac{u_z}{u_*} = \frac{1}{k} \ln\left(\frac{z}{z_0}\right) \tag{1}$$

where u_z (m s^{-1}) is mean wind speed at height z (m), k is the von Kármán constant (0.4), and z_0 is the aerodynamic roughness length (m). Friction velocity is proportional to surface shear stress (T_o [N m^{-2}] = $\rho_a u_*^2$, where ρ_a is atmospheric density [kg m^{-3}]). In the presence of roughness elements of sufficient size and density, Eq. (1) can include a displacement height (Jackson, 1981); but the presence of a displacement height effectively prohibits erosion (Gillette et al., 2006).

The Raupach et al. (1993) model has been successfully applied to a wide range of empirical data representing various scales of measurements from small roughness in wind tunnels to large solid roughness and shrubs in field settings (e.g., Marshall, 1971; Lyles et al., 1974; Gillette and Stockton, 1989; Musick and Gillette, 1990; Wolfe and Nickling, 1996; Musick et al., 1996; Gillies et al., 2006, 2007).

The Raupach et al. (1993) model is defined as:

$$R_t = \frac{u_{*t}}{u_{*s}} = \frac{1}{(1 - m\sigma\lambda)^{0.5}(1 + m\beta\lambda)^{0.5}} \tag{2}$$

where R_t = threshold shear velocity ratio, u_{*t} = threshold shear velocity of bare surface (m s^{-1}), u_{*s} = threshold friction velocity with roughness elements (m s^{-1}), σ = roughness element basal area to frontal area ratio, λ = roughness density, β = ratio of element to surface drag coefficients, m = an empirical constant ranging from 0 to 1 that accounts for the spatial heterogeneity of surface shear stress.

The roughness density (λ) is defined as:

$$\lambda = nbh/S \tag{3}$$

where n = the number of roughness elements occupying the ground area (of the plant community), b = element breadth (m), h = element height (m), and S = ground area (m^2). It should be noted that according to Shao and Yang (2008), the Raupach et al. (1993) model is applicable only to sparse roughness where λ is <0.1.

Calculating λ for vegetation that is shrub- or bush-like is relatively simple, and a number of methods are available including transect methods (e.g., Musick, 1999) and plot-scale measurements (e.g., Gillies et al., 2006, 2007). Lancaster and Baas (1998) estimated λ for salt grass (*Distichilis spicata*) communities by measuring maximum height (h), length of the longest axis (l), length of the perpendicular axis (w), and number of clumps (n) in 1 m^2 quadrats spaced 1 m apart along two 40 m long transects through their measurement sites to estimate λ using:

$$\sum \frac{\{nh\left[\frac{wl}{2}\right]\}}{a} \tag{4}$$

where a is the area of each quadrat (i.e., 1 m^2). The smaller the individual grass plants or sward, which is a population of individual plants, the more logistically difficult it becomes to effectively define and measure the length scales to determine λ for grass type vegetation. It probably can best be estimated using a quadrat technique similar to that used by Lancaster and Baas (1998). Scaling up this kind of measurement procedure to obtain representative regional vegetation roughness characteristics is not logistically feasible and other methods must be developed for that purpose.

In addition to information about the number of elements and their length scales, the Raupach et al. (1993) model requires knowledge of aerodynamic properties of the roughness and intervening surface. The aerodynamic property required is the drag coefficient for the surface and roughness elements. The dimensionless drag coefficient (Cd_s) of a surface can be described by (Priestley, 1959):

$$Cd_s(z) = \frac{\tau_0}{\rho u_z^2} = \frac{u_*^2}{u_z^2} \tag{5}$$

and represents the degree to which the total force of the wind is reduced by drag on the surface as a result of momentum extraction from wind flow. Applying the Raupach et al. (1993) model in sparse vegetation requires a value of Cd_s for the bare intervening surface.

The drag coefficient of a surface-mounted roughness element can be defined as (Raupach, 1992):

$$Cd_s = \frac{F}{(\rho_a A_f u_z^2)} \tag{6}$$

where F is the force (N) exerted on the element by fluid flow and A_f is the element cross sectional or frontal area (m^2). For winds in terrestrial environments, Cd_e for solid elements becomes independent of flow Reynolds number (Re_h) at relatively low wind velocities. Reynolds number here is defined as:

Please cite this article in press as: Shinoda, M., et al. Temperate grasslands as a dust source: Knowledge, uncertainties, and challenges. Aeolian Research (2011), doi:10.1016/j.aeolia.2011.07.001

$$Re_h = \frac{\rho_a u_z h}{\mu} \quad (7)$$

where h is element height, and μ is atmospheric (dynamic) viscosity (N s m^{-2}).

Unlike solid elements, very little information is available on the behavior and aerodynamic properties of different plant types. Work by Wyatt and Nickling (1997) plus Grant and Nickling (1998) demonstrated that drag coefficients of porous vegetation (natural and artificial) are greater than solid element forms with the same physical dimensions. These results were confirmed by Gillies et al. (2000). As a result, use of solid element drag coefficients for vegetative roughness elements would lead to underestimation of their effectiveness to partition shear stress using the Raupach et al. (1993) model. In addition to having drag coefficients greater than their solid element equivalent form, Gillies et al. (2000, 2002) demonstrated that different plant forms can have very different drag curves from those of solid elements, as well as among different plant form types.

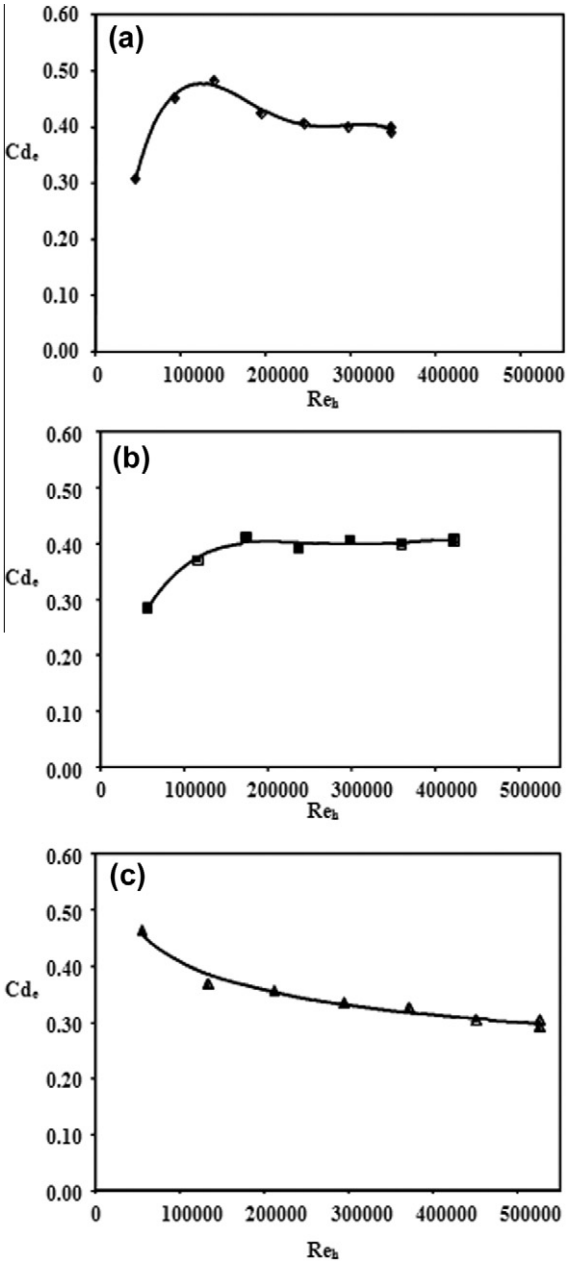

Fig. 5. Drag curve relationships (i.e., Cd_e versus Re_h) for three plant types; (a) small shrub with leaves, (b) small evergreen tree with needles, and (c) grass (after Gillies et al., 2002).

Gillies et al. (2002) presented drag curves (Fig. 5) for three plant types that show, unlike simple solid element forms, complex responses to flow Reynolds numbers through the range of wind speeds that cause wind erosion and dust emissions to occur. The complexity of the Cd_e versus Re_h relationship arises from morphological responses (changing frontal area and porosity) of the plants to the force of the wind. Gillies et al. (2002) observed that shrub-like plants had initially increasing Cd_e as Re_h increased to a maximum, which was associated with a maximization of frontal area by the leaves followed by a gradual decline with further increases in Re_h. For the grass measured by Gillies et al. (2002), Cd_e was observed to decline continually with increasing Re_h, which has important implications for modeling shear stress partition effects in environments like TGs that are dominated by grass cover of varying amounts. In all three types of vegetation, shear stress partitioning can be non-linear, unlike sparsely distributed solid elements where λ is <0.10.

Two studies (Nickling et al., 1999; Gillies et al., 2002) presented drag curves for grasses derived from drag balance measurements to measure the force on vegetation as a function of wind speed in wind tunnel testing. Nickling et al. (1999) measured Cd_e values for dried bunches of salt grass of various widths (0.025 m, 0.05 m, and 0.10 m) and height (0.10 m, 0.15 m, and 0.20 m) combinations. Optical porosity of the salt grass bunches was on average 0.52 (±0.07). Gillies et al. (2002) measured Cd_e for live fountain grass (*Pennisetum setaceum*) approximately 0.45 m high with varying optical porosity (0.34, 0.36, 0.40, 0.43, and 0.51).

The behavior of the Cd_e versus Re_h relationship differs somewhat between these two grass species, specifically for the small diameter (0.025 m and 0.05 m) salt grass clumps compared with the larger 0.1 m diameter salt grass clump and fountain grass. In the case of dry, small-diameter senescent salt grass bunches tested by Nickling et al. (1999), the grass blades were relatively inflexible and Cd_e for an isolated bunch was observed to be relatively invariant and between 0.8 and 0.9 through the range $25{,}000 < Re_h < 250{,}000$. For the larger diameter clumps of salt grass (0.1 m diameter) and fountain grass, Cd_e declines exponentially with increasing Re_h. The salt grass Cd_e decreases much faster with Re_h than the fountain grass, but approach similar values at $Re_h > 200{,}000$ of 0.5 and 0.3 for salt grass and fountain grass, respectively.

The Nickling et al. (1999) study also demonstrated that for groups of grass bunches arranged in a staggered array, total drag on the roughness increased with increasing numbers, but Cd_e decreased as the number of bunches per unit area increased. After addition of sufficient rows of bunches, they observed that the rate of change of additional drag force as Re_h increased became constant and Cd_e stabilized. At this point, protection by aerodynamic properties (if plant form remains unchanged) is at a maximum for that configuration; and additional protection comes from the areal extent of the plant cover. These relationships are, to date, the only drag curve relationships available to estimate shear stress partitioning effects for grasses. Their application would require some knowledge of optical porosity and the physical characteristics of the grass that was on the surface of interest.

In addition to the aerodynamic influence of vegetation on wind erosion processes, vegetation can cover portions of the surface lying prone or prostrate. This contributes to a second means by which entrainment and transport processes are modulated. The effect of prostrate vegetation cover was first examined by Chepil (1944) and later by Siddoway et al. (1965) and Lyles and Allison (1981), with each of these papers reporting that the reduction in erosion varied exponentially with the quantity of surface residue, expressed as weight per unit area and soil type.

Please cite this article in press as: Shinoda, M., et al. Temperate grasslands as a dust source: Knowledge, uncertainties, and challenges. Aeolian Research (2011), doi:10.1016/j.aeolia.2011.07.001

Fryrear (1985) derived a two parameter exponential relationship between the soil loss ratio (SLR; i.e., soil loss from covered soil/soil loss from the same soil that is both bare and flat) and the cover expressed as a percent with the form: $SLR = ae^{-b(\%SC)}$, where %SC is percent surface cover. The Fryrear (1985) model was tested by Leys (1991) who found that the SLR relationship as a function of percent cover overestimated the erosion rate. Leys (1991) also observed that a two parameter model failed to provide meaningful results at low cover levels because as %SC goes to zero, SLR can be greater than one, which is not plausible. Leys (1991) suggested a one parameter exponential model (i.e., $SLR = e^{-b(\%SC)}$) to eliminate this problem while recognizing that this causes a second problem, which is that SLR can never become zero no matter the %SC. In addition, this model gives the same SLR regardless of wind speed, which as Leys (1991) data shows is not the case. Leys (1991) also noted that SLR reaches zero well before there is 100% surface cover. Evaluating the role of surface cover in isolation as a surface characteristic that affords protection to an erodible surface has not been as vigorously pursued as investigations into how aerodynamic properties of surfaces affect wind erosion. One option that will be introduced and discussed in more detail later is to treat surface cover as parameter that modifies saltation efficiency.

The drag partition theory as described above has major limitations and is not readily applicable to wind erosion modeling over TGs. The first limitation lies in the definition of surface roughness elements. It is, in practice, extremely difficult to match a real grassland surface to the idealized surface composed of an underlying smooth surface superposed with roughness elements. Rather, the surface is composed of a variety of roughness elements of different sizes and shapes, which also may alter their form in response to the force of the wind (Gillies et al., 2002). Three difficulties are associated with this problem. First, it is virtually impossible to determine frontal area index with accuracy for extensive areas. Second, a multi-stage drag partition theory needs to be developed in order to estimate shear stress on mobile soil particles. As Shao and Yang (2008) pointed out, the drag partition formulation of Raupach (1992) and Raupach et al. (1993) is valid for cases with small frontal area indices ($\lambda \leqslant 0.1$); and this limitation can be traced back to the supposition hypothesis, which becomes invalid as the density of roughness elements increases. The third difficulty is that unlike solid roughness elements, vegetation can alter its form and thus change drag properties.

The second limitation of the drag partition theory is that it does not take into consideration local flow patterns around roughness elements. It has been observed frequently in field and wind tunnel experiments that a roughness element may generate a vortex in front of it and accelerated flow around it (Sutton and McKenna Neuman, 2008). As a consequence, under certain circumstances, the presence of roughness elements enhances rather than suppresses wind erosion (Fig. 6). In a preliminary numerical study, Yang and Shao (2005) found that for $\lambda \leqslant 0.012$, wind erosion is enhanced by roughness elements due to local turbulence, while for $\lambda \geqslant 0.012$, wind erosion is suppressed by roughness elements due to momentum absorption. While there are quantitative uncertainties in the results of Yang and Shao (2005), the qualitative statement appears to be reasonable.

An alternative but almost identical approach to the above described drag partition is to represent the effect of roughness elements in terms of aerodynamic roughness length, which is a more integrative parameter and relatively easier to estimate. Suppose the overall roughness (roughness elements plus underlying surface) length is z_0, then the profile of wind in the atmospheric boundary layer is approximately logarithmic (Eq. (1)). If the roughness elements are not too closely spaced (i.e., $\lambda < 0.1$), an internal boundary layer would grow behind each individual roughness element. The modified wind profile in the internal boundary layer also follows a logarithmic law. Supposing the roughness length of the underlying surface is z_{00}, it is then possible to express (Marticorena et al., 1997):

$$R_t = 1 - \frac{\ln\left(\frac{z_0}{z_{00}}\right)}{\ln\left[a\left(\frac{\Delta x}{z_{00}}\right)^{0.8}\right]} \tag{8}$$

where R_t is a function of z_0, z_{00}, and Δx (separation between roughness elements). The a term is a function of the roughness density and flow properties; and according to King et al. (2005) based on re-evaluation of Marshall's (1971) data and using the solution proposed by Elliot (1958), is equal to 0.7. Marticorena and Bergametti (1995) had originally calculated in error the value of a to be 0.35. Specifications of these parameters for practical use are not easier than the specification of frontal-area index; and as King et al. (2005) point out, this model applies only to situations of small-scale wakes as the model parameter x is not independently scaled to the size of the roughness but an absolute distance.

Fig. 6. Enhanced local wind erosion due to the presence of roughness elements observed in a wind tunnel experiment conducted by Shao in 1993 (unpublished).

Please cite this article in press as: Shinoda, M., et al. Temperate grasslands as a dust source: Knowledge, uncertainties, and challenges. Aeolian Research (2011), doi:10.1016/j.aeolia.2011.07.001

Table 1
A list of empirical and semi-empirical relationships between roughness length z_0 and frontal area index λ. The references used are L1969 (Lettau, 1969), C1971 (Counihan, 1971), T1993 (Theurer, 1973), MBAG1997 (Marticorena et al., 1997), MGH1998 (Macdonald et al., 1998), and SY2007 (Shao and Yang, 2008).

Reference	Formula for z_0/h	Comment
L1969	0.5λ	$\lambda < 0.2$
C1971	$1.8\lambda - 0.08$	$0.06 < \lambda < 0.15$
T1973	$1.6\lambda(1 - 1.67\eta)$	$\lambda < 0.25$
MBAG1997	$0.48\lambda + 0.001$	$\lambda < 0.11$
	0.0538	$\lambda \geqslant 0.11$
MGH1998	$(1-\frac{d}{h})\exp\left\{-\left[0.5\alpha\frac{C_d}{\kappa^2}(1-\frac{d}{h})\lambda\right]^{-0.5}\right\}$	$\frac{d}{h} = 1 + A^{-\lambda}(\lambda - 1); A \propto 4; \alpha = 0.55$
SY2008	$\frac{z_r - d}{h}\exp\left[-\kappa\sqrt{f_r\lambda(1-\eta)C_r + f_s(1-\eta)C_s + f_c\eta C_c}\right]$	$\frac{d}{h} = \frac{\tau_r}{\tau}\sqrt{\eta} + \frac{\tau_c}{\tau}$

It is not surprising that R_t can be expressed either in terms of λ or z_0, because a close relationship exists between the two quantities. Several empirical or semi-empirical relationships between z_0 and λ have been proposed, as summarized in Table 1.

The schemes of Lettau (1969), Counihan (1971), Theurer (1973), and Marticorena et al. (1997) are empirical expressions derived through fitting to wind-tunnel and field experimental data. These expressions indicate that λ depends linearly on z_0 for surfaces with sparsely distributed roughness elements, according to:

$$\frac{z_0}{h} \propto \lambda \tag{9}$$

where h is the average height of the roughness elements. Such a linear relationship is valid for $\lambda < 0.1$ to ≈ 0.3 depending on the data sets used for fitting. These relationships allow calculation of frontal-area index given the average height of sparsely distributed roughness elements and overall aerodynamic roughness length of the surface.

The dependency of z_0 on λ is in general non-linear. While z_0 increases almost linearly with λ if λ is small, it decreases with λ if λ exceeds a certain limit (Wooding et al., 1973; Hatfield, 1989). The non-linear behavior of the $z_0(\lambda)$ relationship can be seen clearly from the wind-tunnel observations of Hall et al. (1996). As shown in Fig. 7, z_0/h increases with λ for small λ, but drops off after peaking at about $\lambda = 0.15$. Macdonald et al. (1998) proposed expressions that correctly describe the behavior of z_0 over the full range of λ values. In the expression of Macdonald et al. (1998), d is displacement height.

Shao and Yang (2008) argued that τ can be partitioned in general into three terms: the pressure drag, τ_r; the friction drag on the surface, τ_s; and the friction drag on the roughness element, τ_c:

$$\tau = \tau_r + \tau_s + \tau_c$$

$$\tau_r = \rho f_r C_r U^2(1-\eta); \quad \tau_s = \rho f_s C_s U^2(1-\eta); \quad \tau_c = \rho f_c C_c U^2 \eta \tag{10}$$

where C_r, C_s, and C_c are the pressure-drag coefficient, the friction-drag coefficient for the ground surface, and the friction-drag coefficient for the roughness-element surface at zero λ, respectively, and f_r, f_s, and f_c are functions of λ and η (fraction of cover) representing the modifications to C_r, C_s, and C_c arising from the presence of roughness elements. Further, Shao and Yang (2008) suggested that:

$$f_r = \exp\left[-\frac{a_r\lambda}{(1-\eta)^k}\right]; \quad f_s = \exp\left[-\frac{a_s\lambda}{(1-\eta)^k}\right]; \quad f_c = 1 + \left(\frac{C_c}{C_s} - 1\right)\eta \tag{11}$$

with $a_r = 3$, $a_s = 5$, and $k = 0.1$. This formulation of drag partition theory leads to the z_0/h relationship given in Table 1, where z_r is a reference height ($\approx 2h$).

A potentially useful approach to study and characterize grassland wind erosion processes is to conceptualize the surface as three fractions: one of standing grass, η_g; a second of grass lying flat on the surface, η_r; and a third as the fraction of bare soil surface, η_s. The impact of the standing grass is accounted for through drag partition theory and a correction of threshold friction velocity u_{*t}, while the impact of the flat vegetation cover can be accounted for by modifying the saltation equation. The latter situation is equivalent to supply limited saltation. Gillette and Ono (2008) analyzed saltation data and modified the theory of Owen (1964) using a soil-related parameter A that gives the possibility of expressing supply-limited saltation. Shao (2008) argues that the vertically integrated stream-wise flux for supply-limited saltation, $Qslm$, is smaller than or equal to its potential value Q; and a useful theory can be derived based on the assumption of independent saltation. A special case of supply-limited saltation is that a fraction of the surface ($\eta_g + \eta_r$) is not erodible while the remaining fraction of

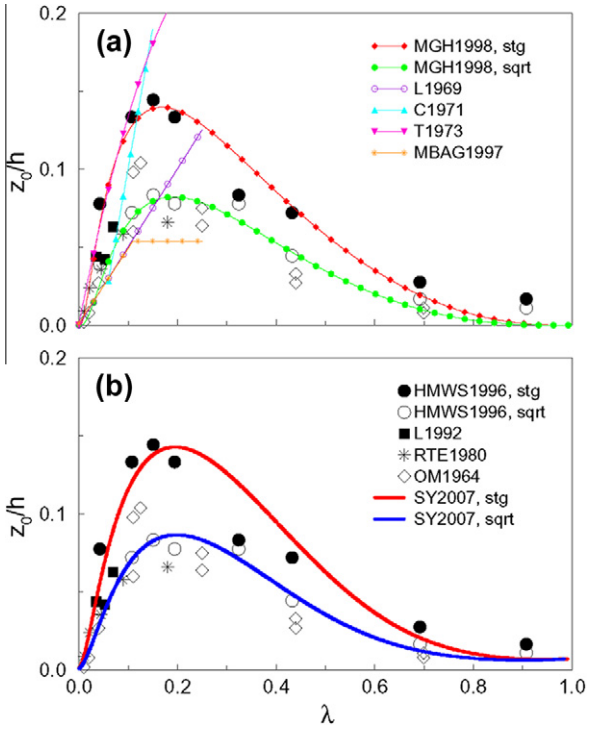

Fig. 7. (a) Comparison of z_0/h estimated using various schemes listed in Table 1 with the wind–tunnel data of Hall et al. (1996), HMWS1996, for the square-array (sqrt) and staggered–array (stg) cases of cubic roughness elements of 0.01 m. The data from Liedtke (1992), L1992, Raupach et al. (1980), RTE1980, and O'Loughlin and MacDonald (1964), OM1964, are also shown for comparison. The estimates of z_0/h using the scheme of Macdonald et al. (1998), MGH1998, are shown. For the staggered- and the square-array cases, $\alpha = 1$ and $\alpha = 0.55$ are used, respectively. (b) A comparison of the scheme of Shao and Yang (2008) with the data. For both the staggered- and square-array cases of HMWS1996, $z_r = 2h$, $z_{00} = 7.5 \times 10^{-4}h$ (or $C_s = 2.57 \times 10^{-3}$), and $z_{00c} = 7.5 \times 10^{-3}h$ (or $C_c = 6.68 \times 10^{-3}$) are set, but with $\beta = 120$ and 80, respectively.

Please cite this article in press as: Shinoda, M., et al. Temperate grasslands as a dust source: Knowledge, uncertainties, and challenges. Aeolian Research (2011), doi:10.1016/j.aeolia.2011.07.001

the surface, η_s is erodible. In this case, the Owen (1964) second hypothesis becomes:

$$\tau_{p0} = \eta_s \rho (u_*^2 - u_{*t}^2) \tag{12}$$

and the Owen saltation equation becomes:

$$Q_{sim} = \eta_s \frac{c\rho}{g} u_*^3 \left(1 - \frac{u_{*t}^2}{u_*^2}\right) \tag{13}$$

Thus, for supply-limited saltation we have:

$$Q_{sim} = \eta S Q \tag{14}$$

In reality, η_s is time-dependent and varies with vegetation cover.

A particularly interesting development in recent years has been deriving wind-erosion parameters based on satellite remote sensing. Chappell et al. (2010) proposed to replace frontal area index with the proportion of shadow, visible at nadir, integrated for all illumination zenith angles for a particular azimuth angle. The shadow proportion depends on geometric anisotropy of surface roughness in common with the aerodynamic roughness length (z_0) (Chappell et al., 2010). There is a direct relationship between the brightness of the surface roughness of previous studies and their measured z_0 (Chappell et al., 2010). There is considerable potential to estimate z_0 frequently over very large areas using the single scattering albedo of the Earth's surface that is readily measured by medium resolution (200–300 m pixels), multi-angle reflectance sensors on airborne and satellite platforms.

Attempts also have been made to estimate z_0 for arid regions using the surface protrusion coefficient. Roujean et al. (1992) suggested that the Bidirectional Reflectance Distribution Function (BRDF) is a combination of zenith reflectance (k_0), surface diffusion (k_1), and volume diffusion (k_2). The protrusion coefficient (PC), defined as the ratio of k_1 to k_0, turns out to be:

$$PC = \frac{k_1}{k_0} \propto \frac{hl}{S} \tag{15}$$

where h and l are, respectively, the average height and average length of the surface protrusions and S is the horizontal surface associated with each protrusion. This implies that PC is proportional to the frontal area index of surface roughness elements and is thus related to z_0. The protrusion coefficient has been retrieved from BRDF data acquired from the Polarization and Directionality of the Earth Reflectance (POLDER-1) radiometer onboard the polar heliosynchronous ADEOS-1 satellite. Marticorena et al. (2004) proposed the following empirical relationship between z_0 and PC:

$$z_0 = a \exp\left(\frac{PC}{b}\right) \tag{16}$$

with $a = 4.859 \times 10^{-2}$ mm and $b = 0.052$. This equation has been used to estimate z_0 over the Sahara, Arabian Peninsula, and desert areas of China and Mongolia. The z_0 values retrieved for various arid areas in China and Mongolia range from less than 10^{-2} mm in the sandy areas of the Taklimakan up to 5 mm in some parts of the Gobi desert. These values agree in general with z_0 estimates based on wind-profile measurements for similar types of surfaces. Note that the vegetation length parameters h and l in Eq. (14) are not static through time and also can effectively change under the influence of applied wind stress.

Based on the above discussions, understanding the aerodynamic and physical controls of grassland vegetation on wind erosion and dust emission processes remains a challenge. Additionally, much of what is known has arisen from small-scale wind tunnel and limited field testing. Scaling known relationships upward to the regional domain remain to be evaluated. This applies to both models for entrainment and transport of sediments as well as aerodynamics of vegetated surfaces. Validation of surface characterization measurements obtained via remote sensing techniques and quantification of their relationship with surface and aerodynamic roughness remain to be undertaken, but remote sensing holds promise as a means to quantify critical parameters affecting dust emissions that cannot be obtained for large regions by other means.

4. Modeling of dust emissions with applications to TGs

Wind erosion models have been under development for the purposes of (1) estimation of wind-erosion intensity and development of guidelines for land conservation, (2) quantification of global and regional dust cycles, and (3) investigation of wind-erosion mechanisms. Models specific for grassland wind-erosion processes are yet to be developed that take into consideration unique characteristics of grasslands, in particular the special roles of vegetation and grazing. This section reviews available modeling approaches and provides guidance for their further development to address TG-specific needs.

4.1. WEQ and WEPS

Wind erosion models for farmland conservation have been under development at the US Department of Agriculture (USDA) for decades. Woodruff and Siddoway (1965) proposed the Wind Erosion Equation (WEQ) to estimate average soil loss due to wind erosion, E (tons/acre/year):

$$E = f(I, K, C, L, V) \tag{17}$$

where I is the soil erodibility factor, K is the soil ridge roughness factor, C is the climate factor, L is the equivalent unsheltered distance across the field along the prevailing wind erosion direction, and V is equivalent vegetative cover. The WEQ estimates E for a field provided that surface conditions represented by these parameters are specified. Feedbacks between wind erosion and land surface conditions are not considered.

Hagen et al. (1996a,b) developed the Wind Erosion Prediction System (WEPS) as a replacement for the WEQ. WEPS is a process-based model for wind-erosion patterns on daily timescales. WEPS consists of seven sub-models, including (1) WEATHER (generates daily atmospheric data), (2) HYDROLOGY (for changes in soil temperature and moisture), (3) SOIL (for changes in the soil properties between management events), (4) CROP (for crop plant growth), (5) DECOMPOSITION (for crop plant decomposition), (6) MANAGEMENT (for step changes in soil and biomass conditions generated from typical management practices such as tillage, planting, harvesting, and irrigation), and (7) EROSION (for wind erosion estimates). WEPS requires four databases for (1) climate, (2) soils, (3) management, and (4) crop and decomposition. An advantage of WEPS is that it simulates both wind erosion and the processes that modify susceptibility of soil to wind erosion.

In WEPS, wind erosion is initiated if $u_* \geqslant u_{*t}$. The duration and intensity of an erosion event are then determined by considering the wind speed distribution and evolution of the surface condition. A stochastic model is used to generate weather parameters (e.g., wind speed), which drive the wind erosion model (Skidmore and Tatarko, 1990). For this purpose, the weather generator requires a database of wind statistics for a given region. As no real weather data are used, WEPS does not simulate individual wind-erosion events.

WEPS includes a detailed treatment of wind-erosion processes, including calculation of friction velocities, threshold friction velocities, and soil loss/deposition. Friction velocity is estimated from mean wind speed using the logarithmic wind profile and aerodynamic roughness length, z_0. Attention has been paid to derive z_0 in relation to farmland ridge spacing and height plus the biomass

Please cite this article in press as: Shinoda, M., et al. Temperate grasslands as a dust source: Knowledge, uncertainties, and challenges. Aeolian Research (2011), doi:10.1016/j.aeolia.2011.07.001

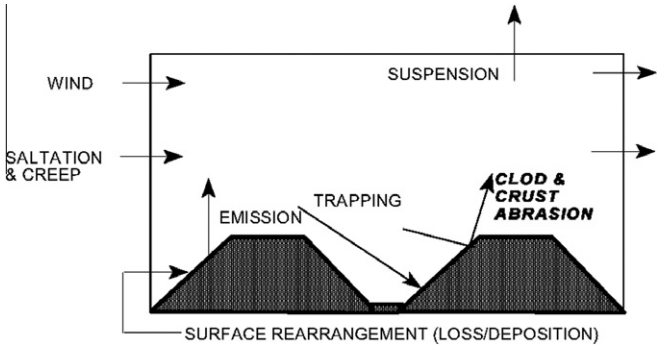

Fig. 8. Diagram of control volume with a ridged bare soil illustrating the sources and sinks used in the WEPS EROSION submodel.

sheltering effect. The basic ideas of determining aerodynamic roughness and sheltering effect are similar to those presented in Section 3, but specific formulations are somewhat different.

WEPS is based on the mass conservation of saltating (including creep) materials (Fig. 8). The equation for mass conservation of saltation mass, M, on a two-dimensional (2D) rectangular simulation region can be written as:

$$\frac{\partial M}{\partial t} = \frac{\partial Q}{\partial x} + G_{en} + G_{an} - G_{tp} - G_{ss} \tag{18}$$

where Q is streamwise saltation flux in the direction of x aligned with wind, G_{en} is emission from loose soil, G_{an} is emission due to abrasion, G_{tp} is deposition due to trapping, and G_{ss} is suspension. A similar approach is taken to model suspended dust mass.

Thus, WEPS ventures to estimate a number of terms such as Q, G_{en}, G_{an}, G_{tp}, and G_{ss}, which are difficult to compute. The disadvantage of this approach, however, is that the model becomes excessively complex and involves too many empirical constants, which are difficult to determine for areas other than southwest USA where data are available thanks to many years of observational effort. In contrast, most other wind-erosion models assume equilibrium saltation, so that:

$$\frac{\partial Q}{\partial x} = 0 \tag{19}$$

and compute Q using the Bagnold–Owen type of saltation equations (Shao, 2000). This is a much simpler approach.

4.2. Integrated wind-erosion models

The need to understand the role of dust in the climate system has prompted intensive development of dust models since the late 1980s. This started with modeling transport of dust similar to air pollutants (Pilinis and Seinfeld, 1987; Westphal et al., 1988). In early dust models, crude dust emission schemes were used. It was soon realized that dust models must properly parameterize the microscopic physics of wind erosion. Physically-based, wind-erosion models with varying degrees of complexity were then developed (e.g., Marticorena and Bergametti, 1995; Shao et al., 1996). Since then, many regional dust models have been constructed and applied to major wind erosion regions around the world, including Antarctica (Genthon, 1992), the Mediterranean (Nickovic and Dobricic, 1996), the United States (Binkowski and Shankar, 1995), the Saharan desert (Marticorena et al., 1997; Schulz et al., 1998), Australia (Shao and Leslie, 1997; Shao et al., 2007), and Asia (Shao et al., 2003; Uno et al., 2005). Numerous modeling studies have been carried out on Saharan dust storms (Pérez et al., 2006; Heinold et al., 2008; Todd et al., 2008; Menut et al., 2009; Bou Karam et al., 2009; Schepanski et al., 2009; Reinfried et al., 2009; Cavazos et al., 2009; Shao et al., 2010). Global dust models also have been under development since the 1990s (Tegen and Fung, 1994, 1995; Zender et al., 2003; Ginoux et al., 2004; Tanaka and Chiba, 2006) and at the same time, dust models with very high spatial resolution have been developed to model mesoscale dust events (Seino et al., 2005; Vogel et al., 2006).

The common structure of integrated dust models is illustrated in Fig. 9. Such a system includes an atmospheric host model that simulates atmospheric dynamic and physical processes such as advection, convection, turbulent diffusion, radiation, and clouds as well as land-, ocean- and ice-surface parameterizations. The core module of the system is parameterization of the emission,

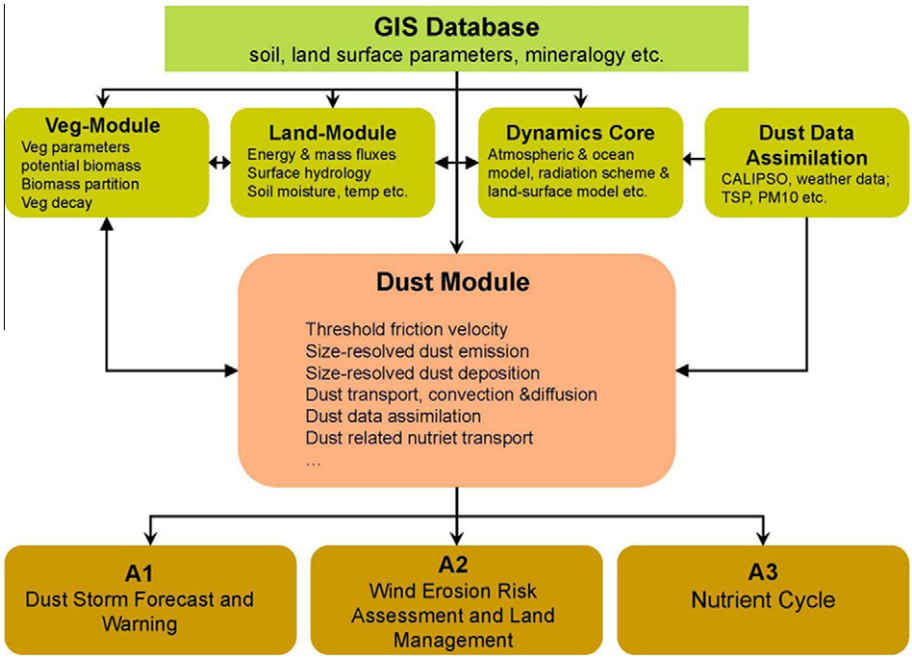

Fig. 9. Common structure of an integrated wind-erosion modelling system.

Please cite this article in press as: Shinoda, M., et al. Temperate grasslands as a dust source: Knowledge, uncertainties, and challenges. Aeolian Research (2011), doi:10.1016/j.aeolia.2011.07.001

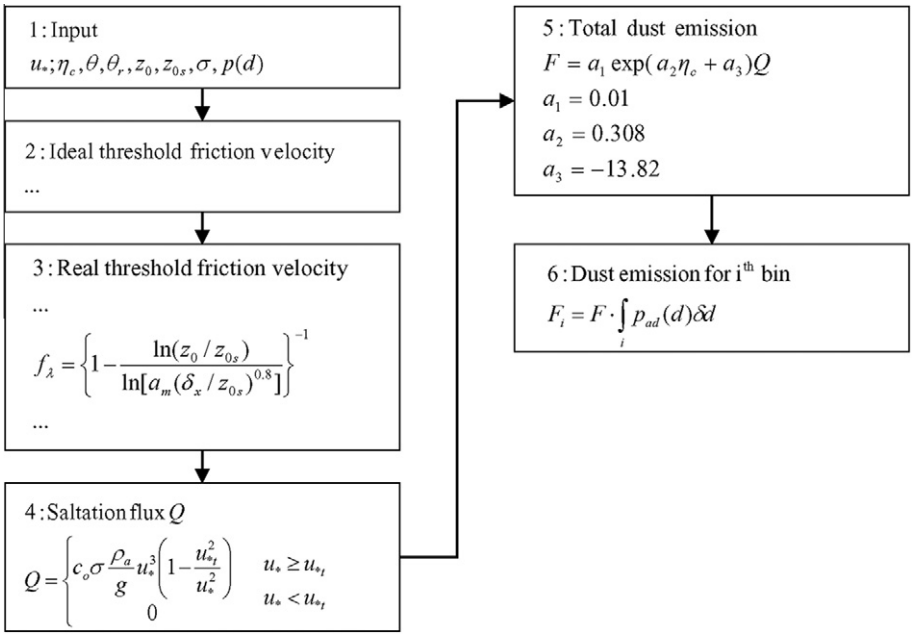

Fig. 10. The structure of the wind-erosion scheme proposed by Marticorena and Bergametti (1995).

Table 2
A summary of three dust-emission schemes.

Scheme	Ref.	Expression	Comments
I	GP88	$F = \alpha_g u_*^n(1-u_{*t}/u_*)$	Hypothesis; not spectral
II	MB95	$F/Q = Q_1\exp(a_2\eta_c - a_3)$	Empirical, a_1 = 100, a_2 = 0.31, a_3 = 13.82; Not spectral
III	S04	$F(d_i;d_s) = c_y\eta_{fi}[(1-\gamma)+\gamma\sigma_p](1+\sigma_m)\frac{Q(d_s)g}{u_*^2}$ $F(d_i) = \int_{d1}^{d2}F(d_i;d_s)p_s(d)\delta d; F = \sum_{i=1}^{I}F(d_i)$	Theory; spectral

GP88: Gillette and Passi, 1988; MB95: Marticorena and Bergametti, 1995; S04: Shao, 2004.

transport, deposition, and transformation of soil particles of various sizes. Specific parameter data sets are required for characterizing land-surface properties, which commonly are manipulated using a geographic information system (GIS).

With increased availability of dust concentration measurements derived from surface weather stations (Kurosaki and Mikami, 2005), air-quality monitoring stations (Leys et al., 2008), lidar networks (Sugimoto et al., 2003, 2006), and through satellite remote sensing, the technique of data assimilation has been applied increasingly to improve accuracy of dust predictions. Yumimoto et al. (2008) used the four-dimensional variational (4DVAR) technique to model Asian dust storms by assimilating the lidar extinction coefficient into the RAMS/CFORS model for adjoint inversion of dust emission. Ensemble Kalman filters (Sekiyama et al., 2010) are used in conjunction with the MASINGER model for global dust modeling (Tanaka and Chiba, 2005). Assimilation of the CALIOP/

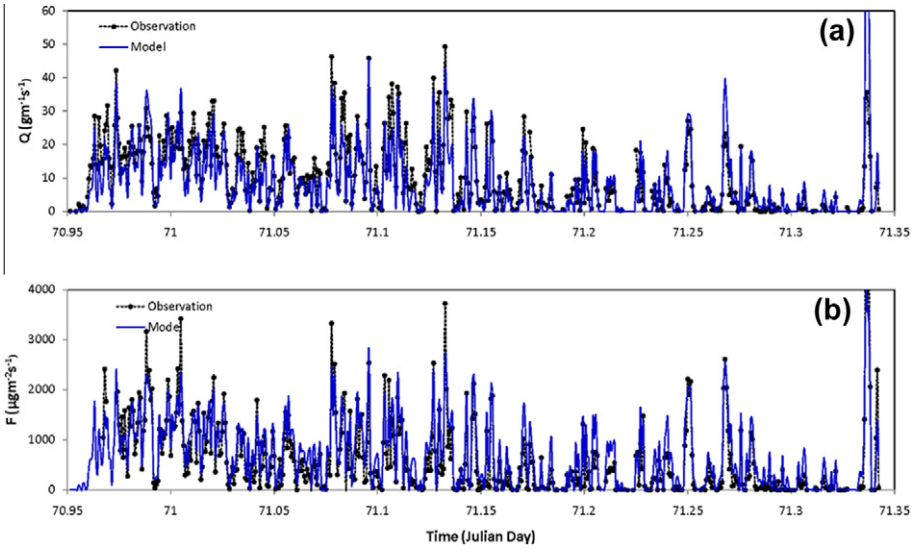

Fig. 11. Comparison of the simulated sand drift using the Shao (2004) wind-erosion scheme with the JADE measurements (a) and of the simulated dust emission with measurements (b).

Please cite this article in press as: Shinoda, M., et al. Temperate grasslands as a dust source: Knowledge, uncertainties, and challenges. Aeolian Research (2011), doi:10.1016/j.aeolia.2011.07.001

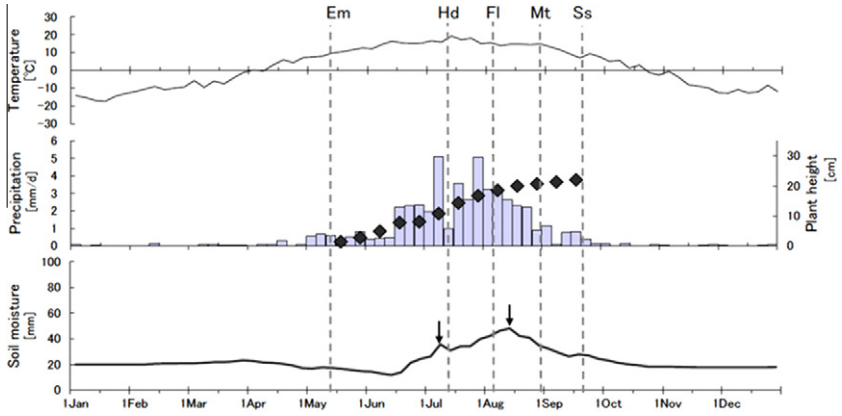

Fig. 12. Climatological seasonal changes of five-day-based temperature (°C), precipitation (bar, mm/d), modeled soil moisture in the top 50 cm soil layer (mm), plant height (diamond, cm), and phenological phenomena in a fenced area (vertical dashed lines, Em to Ss) for Arvaikheer (the typical steppe) (Shinoda et al., 2007). The climatological values and phenological dates were averaged for available years. The arrows denote double peaks of soil moisture. Phenological phenomena such as emergence (hereafter referred to as Em), heading (Hd), flowering (Fl), maturity (Mt), and senescence (Ss) are also indicated.

CALIPSO data made possible the modeling of global dust circulation (Uno et al., 2009).

The starting point of a dust-transport scheme is the dust concentration equation:

$$\frac{\partial c}{\partial t}+u\frac{\partial c}{\partial x}+v\frac{\partial c}{\partial y}+(w-w_t)\frac{\partial c}{\partial z}=K\nabla^2 c+S_r+S_c \tag{20}$$

for different particle size bins (1–2, 2–4, 4–8 μm, etc.). In Eq. (20), t is time, x and y are horizontal distances; z is height; c is dust concentration; K is particle eddy diffusivity; S_r represents wet removal and S_c subgrid convection; u, v, and w are wind velocity components; and w_t is particle terminal velocity. Eq. (20) is solved subject to the surface-boundary condition:

$$\rho(w-w_t)c-\rho K\frac{\partial c}{\partial z}=F \tag{21}$$

where ρ is air density and F is net dust flux at the surface.

Entrainments of sand and dust are parameterized using a wind-erosion scheme. The quantity that represents sand motion is the stream-wise saltation flux Q (kg m^{-1} s^{-1}), while that for dust motion is vertical dust flux, F (kg m^{-2} s^{-1}). A wind-erosion scheme predicts Q and F using a small number of parameters to represent the relevant environmental factors. Fig. 10 illustrates the wind-erosion scheme proposed by Marticorena and Bergametti (1995). The quantity that drives the wind-erosion scheme is u_*. Shao et al. (1996), Alfaro and Gomes (2001), Zender et al. (2003), and Shao (2004) also have proposed wind-erosion schemes.

In most models, Q is computed using the Bagnold–Owen equation or its variations (Shao, 2000). Dust-emission schemes have been proposed by Shao et al. (1993), Marticorena and Bergametti (1995), Alfaro and Gomes (2001), and Shao (2004). Table 2 lists three such schemes. Scheme-I assumes a $F\propto u_*^4$ relationship, and α_g is an empirical coefficient with the dimensions of $\mathrm{M\,L^{-6}\,T^3}$ e.g., μg m^{-6} s^3. The scheme is popular due its simple formulation, but it is not simple to estimate α_g, and there are no guidelines for its specification. Scheme-II assumes that the ratio F/Q is a function of clay percentage η_c. The dimensions of F/Q are (m^{-1}); and a_1, a_2, and a_3 are empirical coefficients. In Scheme-III, both saltation bombardment and aggregate disintegration are considered. The scheme is spectral, because $F(d_i, d_s)$, the emission of dust of size d_i generated by the saltation of sand of size d_s is directly computed. In the scheme, c_y is a coefficient, γ is a weighting function, σ_p is the ratio between free and aggregated dust, and σ_m is bombardment efficiency. The scheme reflects the fact that dust emission is proportional to stream-wise saltation flux, but proportionality depends on soil texture and binding characteristics. The soil and land-surface data required by the scheme are not yet widely available (e.g., the parent soil particle size distribution (psd)).

Most wind-erosion schemes are not well validated due to lack of observations. Shao et al. (2010) tested the wind-erosion model of Shao (2004) against the Japan–Australia Dust Experiment (JADE) data collected by Ishizuka et al. (2008) on an Australian farm and demonstrated good performance of the model in estimates of both Q and F (Fig. 11).

4.3. Vegetation modeling

Existing dust models do not have sufficient capability in modeling vegetation growth and decay, which play a major role in TG aeolian processes. Fig. 12 shows observed seasonal changes of

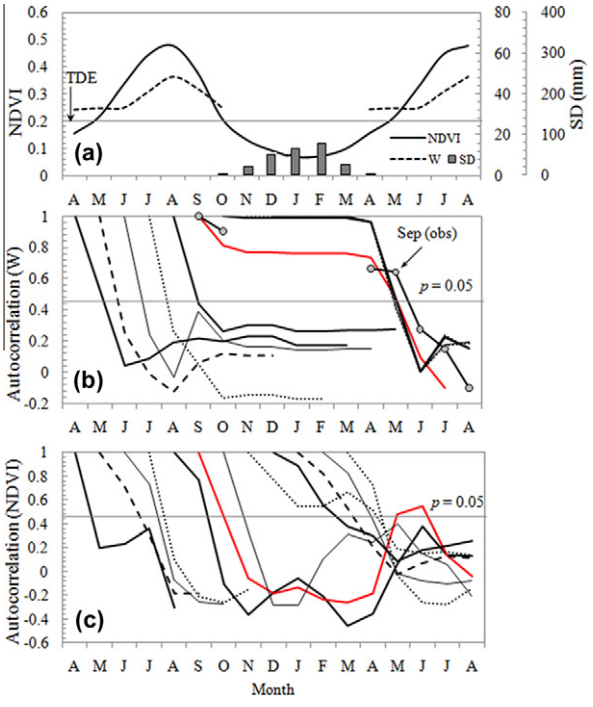

Fig. 13. (a) Climatological (1986–2005) seasonal changes in W_o (mm), NDVI, and SD (mm) for Underkhaan in the steppe and autocorrelations of (b) W_o (only for the reference of September, circle) and W_m, and (c) NDVI using each month as references. The red lines indicate autocorrelations of W_m (b) and NDVI (c) with the reference of September. TDE represents the threshold of dust emission (Kimura et al., 2009). The horizontal thin lines in b and c denote the 5% significance level.

plant height and phenology of *Stipa* spp. (one of the dominant species in the Mongolian steppe) together with those of temperature, soil moisture, and precipitation (Shinoda et al., 2007). The plant observations were made in a fenced area without the influence of grazing, and thus represent the natural state of vegetation growth. As shown, soil moisture exhibits a slight increase during early April due to snowmelt in conjunction with increased temperature. Temperatures at this time are still too low (near 0 °C), however, for plant emergence; and soil moisture due to snowmelt quickly evaporates. Plants respond quickly to summer rain, however, with heading occurring near the first peak of soil moisture, which marks a shift from the vegetative growth to reproductive phase. Heading is defined as the developmental stage of a grass plant from initial emergence of the inflorescence from the boot until the inflorescence is fully exerted (Barnes and Beard, 1992). The plants senescence in September after obtaining their maximum height. This is followed by a period of decay. Over grazing areas, this cycle of vegetation growth and decay is disturbed by animals in varying degrees all year round.

To effectively model aeolian processes under this cycle of vegetative growth and decay, consideration must be given to the effect caused by residual plant components that remain from the previous growing season. In wind-erosion models, it is desirable to consider the natural growth-decay cycles of different vegetative species as well as the effect of grazing on these cycles. Some existing vegetation models can reasonably simulate plant growth, but the decay process rarely has been highlighted in previous studies and deserves better attention in future modeling efforts.

The response of vegetation growth and decay to soil moisture produces an effect on wind erosion activities that can persist for many months. Fig. 13 presents autocorrelations of year-to-year anomalies (from the long-term average) in soil moisture and NDVI along with their seasonal changes for a case study in the Mongolian steppe (unpublished data). Both model simulation and observations show that soil moisture anomalies are significantly autocorrelated during a period of several months (e.g., the model-simulated soil moisture anomaly, W_m in September or later remains significantly autocorrelated until May, expanding during the dust season (Fig. 13b). Similar correlations are found for observed soil moisture (W_o), although these data were interrupted in winter months due to difficulties in sampling when the soil was frozen. In general, there are two interruptions of the soil moisture memory (e.g., autocorrelations): between August and September and between May and June of the following year. Alternatively, the autocorrelation of NDVI from September (also from October) drops abruptly during winter, probably because snow cover masks the anomalies (Fig. 13c). The autocorrelation recovers during May and July of the following year in conjunction with disappearance of snow cover. Similar autocorrelations were identified over the wide area of the Mongolian steppe (Shinoda and Nandintsetseg, 2011). Based on the results presented in Fig. 13 in this TG area of Mongolia, dust emission is very likely to occur during April–May when NDVI drops below the threshold of 0.2, as indicated by the results of Kimura et al. (2009).

Shinoda et al. (2010a) carried out an intensive field experiment at a steppe site in Mongolia during spring 2008 under the joint Japan–Mongolia–USA project Dust-Vegetation Interaction Experiment (DUVEX). They found that the wind erosion threshold wind speed was 8.9 m s^{-1} at 1.54 m above ground level (AGL) for a sandy land surface with only 7.2% vegetation cover of dead leaves, a small roughness length (0.0058 m), and little soil moisture (water content in soil layer 0–5 mm, 0.002 g g^{-1}). The amount of dust emission in this area depends on vegetation cover from 0% to 20% (Kimura et al., 2009). Shinoda et al. (2010a) suggested that the three-year continuous severe drought preceding the spring of 2008 had a deleterious impact on spring vegetation (i.e., phytomass) and affected species composition. Whether the species are palatable to grazing animals or not is an important factor for determining how much phytomass remains during spring after the grazing. Such subtle changes in vegetation during spring need to be reasonably well simulated in order to predict land-surface conditions for dust production.

4.4. Future grassland wind-erosion modeling system

As summarized in the previous sections, integrated wind-erosion modeling systems that couple models of atmospheric, land-surface, and aeolian processes with dust observations and land-surface parameter databases already exist. In these modeling systems, land-surface conditions such as soil texture, soil moisture, vegetation cover, and roughness elements have been taken into consideration with varying degrees of sophistication. These parameters vary in time, are spatially heterogeneous, and their specifications along with quantification of their accuracy have proven to be difficult. Since grassland wind erosion strongly depends on vegetation cover, substantial development of existing wind-erosion models is necessary for such models to be applicable to grassland wind-erosion processes and to be useful for grassland management practices. The following tasks stand out as key issues that must be tackled in the next stage of model development:

- Vegetation growth and decay.
- Impacts of grazing and cultivation.
- Data assimilation, with a focus on soil moisture and vegetation.
- Coupling vegetation model with wind-erosion model.
- Establishment of a grassland aeolian database.

4.4.1. Vegetation growth and decay

Development of plant-growth models and land-surface models is important to wind-erosion research. Sophisticated land-surface models already exist, which allow modeling of the variation of land-surface quantities, such as snow cover, soil moisture, and soil temperature. Grassland and grazing models have been developed by the ecological research community. For example, Wiegand et al. (2008a) summarized a variety of grassland models for temporal and spatial grassland dynamics, diversity, productivity, water dynamics, and nutrient cycles. In relation to aeolian studies, the dominant question is how to manage grasslands for maximal and sustainable grazing, while minimizing erosional losses. Coffin and Lauenroth (1989) developed a spatially explicit gap dynamics simulation model (STEPPE) to evaluate the effects of disturbances at the landscape scale. Their model simulates establishment, growth, and death of individual grass plants on a small plot (~0.1 m^2) through time. Peters (2002) further developed STEPPE to an individual-based gap dynamics model (ECOTONE) for prediction of the effects of climatic fluctuations and other disturbances on regional patterns of vegetation dynamics. Grazing models are an integral part of grassland research and vary to a large degree depending on purpose, scale, and complexity (Wiegand et al., 2008b). Process-based ecosystem models that describe plant growth, soil water, or carbon fluxes have a long tradition. In recent years, researchers are increasingly using individual-based and spatially-explicit (IBSE) models to investigate the processes of desertification and rehabilitation of grassland vegetation, in particular the long-term effect of grazing and climatic fluctuations on vegetation dynamics. IBSE models can be coupled with land-surface models to simulate the processes of seed production, germination, establishment, competition and facilitation, growth, and mortality for the plants. Land-surface parameters required by the IBSE models can be derived from satellite remote sensing.

A crop model has been implemented in WEPS, but not as far as we know into any other wind-erosion modeling systems. The

Please cite this article in press as: Shinoda, M., et al. Temperate grasslands as a dust source: Knowledge, uncertainties, and challenges. Aeolian Research (2011), doi:10.1016/j.aeolia.2011.07.001

model consists of crop parameters for calculating leaf and stem areas and partitioning aboveground biomass into leaf, stem, and reproductive organs, as well as stress- and nutrient-related parameters. The model then deals with phonological development based on the growing-degree-day (GDD) accumulation. For each crop, the potential GDDs from planting to maturity and relative GDDs from planting to emergence, to the beginnings of the reproductive phase and leaf senescence are given. After plant emergence (6% GDD accumulation from date of planting), the potential biomass produced daily is then calculated by multiplying the intercepted light. The daily produced biomass is partitioned to roots and aboveground plant parts to allow estimates of leaf area and plant height. Potential growth and yield are seldom achieved because of stress caused by suboptimal conditions. The plant-growth model adjusts daily biomass and area growth for water, temperature, and nutrient stresses. It is pragmatic to adapt such simple crop models for grassland vegetation and integrate them into the framework of wind-erosion models.

4.4.2. Model and data assimilation (with a focus on soil moisture and vegetation)

Reliable soil moisture data are necessary for grassland vegetation modeling. Historical records of soil moisture content measured in situ are available for few regions in the world and often represent very short periods (Robock et al., 2000); but a unique long-term, quality-controlled data set recently has been established for Mongolia (Nandintsetseg and Shinoda, 2010). For extensive areas, soil moisture can be obtained from coupled atmospheric-hydrological modeling. Land surface models have made such coupled modeling possible (Dickinson et al., 1993). Hydrological simulations are associated with errors that arise from inadequacies in model physics, parameters, forcing data, and initial conditions, which propagate and amplify due to non-linear terms of the model. Data assimilation can be used to reduce these errors by combining model estimates and measurements to achieve optimal predictions. Data assimilation has been implemented most successfully in numerical weather forecasts; and, in recent years, it also has been increasingly applied to surface hydrological modeling. For a future grassland wind-erosion modeling system, we also should emphasise assimilation of satellite data for improved soil moisture and temperature prediction (Walker and Houser, 2001; Reichle et al., 2002; Pan and Wood, 2006).

Land-surface data assimilation is now feasible, as the availability, resolution, and quality of remotely sensed soil moisture and temperature across large areas continue to improve. For example, the Advanced Scatterometer (ASCAT) soil moisture service has been operational in European Organisation for the Exploitation of Meteorological Satellites (EUMETSAT) since December 2008, and is projected to provide soil moisture data until at least 2020 (Scipal et al., 2009). The newest satellite soil moisture data also can be obtained from the Soil Moisture and Ocean Salinity Mission (SMOS) from 2010 onward, with an accuracy of 0.035 $m^3\ m^{-3}$, spatial resolution of 60 km, and temporal resolution of three days. Onboard the Chinese satellite FY3 (launched in 2008) is a 10 GHz microwave radiometer for soil moisture observations. The US Soil Moisture Active and Passive (SMAP) mission (planned for launch in 2010–2013) will enable remote sensing of soil moisture with a resolution down to 10 km. Surface soil temperature, T_s, is one of the most reliable quantities retrieved from satellite observations (e.g., from window channels of AVHRR on board many operational polar orbiting satellites). As T_s is sensitive to soil moisture, T_s can be assimilated to achieve better soil moisture estimates (Crow and Wood, 2003).

Several data assimilation methods exist including Kalman filter (KF) and four-dimensional variational (4D-Var) data assimilation. The 4D-Var technique is more difficult to implement, as it requires the adjoint of the tangent linear model; thus the KF approach is more popular. A KF is suitable for linear systems, which takes into account uncertainties in the modeled and measured state variables and produces optimal estimates of the state variables as weighted averages. For non-linear systems, an extended KF (EKF) is better suited. In both KF and EKF, uncertainties of the state variables (error covariance matrix) are estimated explicitly through the "error-covariance equations," an advantage over the 4D-Var technique. In EKF, the system and/or measurement equations are linearized locally, but not the error-covariance equations directly (Crosson et al., 2002). An alternative is Ensemble Kalman Filter (EnKF), which uses an ensemble of predictions to estimate the gain and error covariance matrix. Also, multi-scale KF (MKF) has been used (Parada and Liang, 2008).

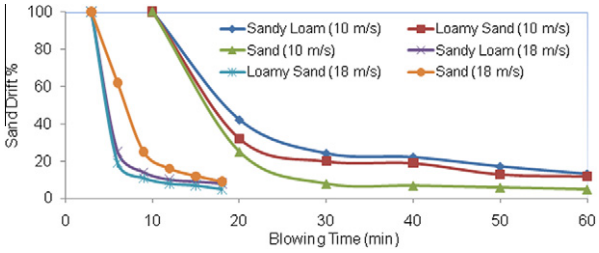

Fig. 14. Decay of sand drift with time for three different soils (sandy loam, loamy sand, and sand) and two erosive wind velocities (10 and 18 m s^{-1}; data from Liu et al., 2003).

Hydrological data assimilation is still at the experimental stage, and many problems require further research. One limitation is the difficulty in estimation of error propagation in the non-linear system of the land-surface model. Then the Gaussian error assumption, which is the basis of many data assimilation methods, breaks down for strongly non-linear problems. Also, many technical problems must be overcome. For instance, assimilation of composite coarse resolution satellite data to continuous fine resolution model simulations needs to be addressed.

Likewise, satellite remote sensing provides a powerful tool for assessment of grassland surface cover, which can be assimilated into grassland vegetation models. Because TG is a relatively simple ecosystem, remote sensing is particularly advantageous for studying vegetation dynamics. NDVI is a good indicator of photosynthesis; and with broad spatial coverage and high temporal resolution, NDVI data sets are increasingly used for monitoring assessments of terrestrial vegetation conditions on regional and global scales, including NPP (Paruelo et al., 1997), vegetation coverage (Los et al., 2001), biomass (Dong et al., 2003), and phenology (Moulin et al., 1997). Piao et al. (2006) analyzed the temporal change of NDVI for TGs in China and its correlation with climatic variables during the period 1982–1999. The latter authors found that average NDVI of the study area increased at rates of 0.5% yr^{-1} for the growing season (April–October), 0.61% yr^{-1} for spring (April and May), 0.49% yr^{-1} for summer (June–August), and 0.6% yr^{-1} for autumn (September and October) during the study period.

4.4.3. Supply limited wind erosion

Most wind-erosion models assume the supply of erodible soil is unlimited. This assumption is only reasonable for sandy soils but is unrealistic for grasslands and results in over prediction of sand drift and dust emission with time. Wind erosion over grasslands is mostly supply limited. Liu et al. (2003) carried out wind tunnel tests of grassland soil surfaces and found that soil loss was a function of blowing time of erosive winds. Wind erosion is most intense during a short initial blowing period and then decreases with time. The rate of sand drift decay appears to be exponential but depends on wind speed and soil type, as shown in Fig. 14.

Please cite this article in press as: Shinoda, M., et al. Temperate grasslands as a dust source: Knowledge, uncertainties, and challenges. Aeolian Research (2011), doi:10.1016/j.aeolia.2011.07.001

Table 3
Estimated log–normal, size-distribution parameters for Chinese desert soils. Also listed are the mean values of $\gamma_b = F/Q$ (Marticorena et al., 1997) for the different soils.

Sample	Clay	Silt	Sand	USDA	Mode1			Mode2			γ_b
	(%)	(%)	(%)		w_1	D_1	σ_1	w_2	D_2	σ_2	(10^{-4} m^{-1})
Taklimakan & Kumtaq	2.0	10.7	87.8	S	0.97	84	1.34	0.03	442	1.42	0.185
East Xinjiang	9.9	34.7	55.3	SL	0.29	90	1.24	0.71	293	1.66	2.120
Gurban Tunggut	3.6	13.5	82.0	LS	0.36	94	1.12	0.64	170	1.69	0.304
Badain Jaran & Ulan Buh	3.4	8.6	88.2	S	0.52	97	1.30	0.48	316	1.59	0.286
Tengger & Kubqi	2.6	7.3	90.7	S	0.72	120	1.48	0.28	322	1.29	0.223
Hexi Corridor	4.8	14.8	80.6	LS	0.40	97	1.26	0.60	386	1.59	0.440
Gobi (Inner Mongolia)	11.9	34.1	53.0	SL	0.42	86	1.38	0.58	457	1.74	3.930
Mu Us	1.6	7.7	90.2	S	0.35	99	1.17	0.65	330	1.37	0.164
Horqin								1.00	315	1.29	0.164
Loess								1.00	65	1.28	19
Sandy loess								1.00	74	1.17	19

Similar observations were made in the Japan–Australian Dust Experiment (JADE) by Mikami et al. (2010). The decay function for different erosive wind velocities and soil types needs to be thoroughly investigated and taken into consideration in wind-erosion models. Liu et al. (2003) argued that the decrease in soil loss with successive exposures was due to emergence of larger soil aggregates on the soil surface, which produce a sheltering effect. This is a plausible explanation, but probably not the only one.

4.4.4. Establishment of grassland aeolian database

Land-surface data parameters are required to quantify the grassland land-surface properties that affect wind erosion, such as the capacity of soil to release dust and the threshold friction velocity for erosion to take place. In the context of wind-erosion modeling, land-surface parameters can be divided into the following three categories:

- Category 1: parameters for specifying soil properties, such as soil texture, soil-salt content, soil-binding strength (either binding energy or soil plastic pressure depending on dust scheme), etc.
- Category 2: parameters for specifying surface aerodynamic properties, such as frontal-area index, erodible fraction, roughness length, etc.
- Category 3: parameters related to soil thermal and hydraulic properties required by land-surface modeling.

Parametric databases for wind erosion modeling in general, and grasslands in particular, are poorly established. For example, soil texture is an essential parameter for wind-erosion modeling, but soil texture data for grasslands are difficult to find or are of poor quality. Nevertheless, Mei et al. (2004) analysed surface-soil samples collected in the Chinese desert areas including the Gobi (in Inner Mongolia), Gurban Tungut, East Xinjiang, Taklimakan, Ulan Buh, Mu Us, Hexi Corridor, Tengger, and Horqin (sandy land). Their soil samples were dry sieved into 10 size classes (40, 40–63, 63–80, 80–100, 100–125, 125–250, 250–500, 500–800, 800–1000, and 1000–2000 μm) and the psds fitted with two log-normal distributions, representing a fine mode and a coarse mode:

$$d \times p(d) = \sum_{j=1}^{N} \frac{w_j}{\sqrt{2\pi}\sigma_j} \exp\left[-\frac{(\ln d - \ln D_j)^2}{2\sigma_j^2}\right] \quad (22)$$

where $p(d)$ is psd, w_j is the weight for the jth mode of the particle-size distribution, and D_j and σ_j are parameters for the log-normal distribution of the jth mode. Additional soil particle-size data for the Badain Jaran desert, Kubqi desert, and Otin Daq and Hulun Buir sandy lands can be found in Yang et al. (2001), although their analyses have fewer particle-size classes and a low resolution for the size range between 100 and 700 μm. The fitted parameters (i.e., w_j, D_j, and σ_j) are summarised in Table 3. Medians of the fine mode, D_1, are consistent among the samples from various deserts. The medians of the coarse mode, D_2, exhibit considerable variation. Mass fractions of the fine and coarse modes, w_1 and w_2, vary significantly among the samples. For example, the mass fraction of the fine mode is 0.97 for the Taklimakan but 0.42 for the Gobi site. The above data reveal that soil psd has considerable heterogeneity. There are large differences in psds even among soils of the same texture. The amount of soil particle-size data currently available is far from sufficient for reliable grassland wind-erosion modeling.

In addition to psd data, serious consideration should be given to collecting soil organic carbon and other mineralogical parameters for TGs and other areas as information on carbon cycling in soils is limited. The dominant soils in TGs are Mollisols with a relatively thick, dark brown to black surface horizon that is rich in organic matter (Arichibold, 1995). The mollic epipedon is organic-rich surface horizon that forms in the presence of bivalent cations, particularly calcium (USDA, 1999). The organic-rich surface horizon is thought to be formed mainly through the underground decomposition of organic residues in the presence of these cations. Wind erosion preferentially depletes organic matter from the top soil of TG and plays an important role in the regional and global carbon cycle. In recent years, the role of wind erosion on the carbon cycle has attracted attention (Hoffmann et al., 2008b).

5. Monitoring

As we have described in previous sections, when vegetation is degraded followed by effects such as overcultivation and overgrazing, sheltering volume and area are decreased. This alters partitioning of friction drag from roughness elements to the ground surface. Thus, dust flux from the surface can increase. In order to understand these physical processes and improve dust emission schemes to be more realistic under sparse vegetation conditions, monitoring of dust emission processes over temperate and/or sparse grassland is needed. The measurements must be made with sufficient particle size and time resolutions to more fully characterize the physical relationships and supply the data that are required for validation of the scheme. To date, most monitoring of dust emission processes has been carried out in deserts, arid lands, and fallow land without vegetation (e.g., Gillette et al, 1997; Ishizuka et al, 2008). Only a few studies aimed at understanding vegetation effects on dust emission have been made on a sparsely vegetated land surfaces (e.g., Marticorena et al., 2010; Shinoda et al., 2010a). In the following section, we will discuss technical requirements for monitoring dust emission processes on TGs and elsewhere. These techniques will be demonstrated by referencing some pioneering studies undertaken in northeastern Asia.

Please cite this article in press as: Shinoda, M., et al. Temperate grasslands as a dust source: Knowledge, uncertainties, and challenges. Aeolian Research (2011), doi:10.1016/j.aeolia.2011.07.001

5.1. Requirements for dust monitoring over TGs

5.1.1. Monitoring parameters

In order to collect required information on dust emission from TGs, monitoring parameters that characterize the conditions of the atmosphere, soil physical properties, and vegetation are needed. The primary driving force for the emission process is surface shear stress that is expressed as a function of friction velocity u_* (i.e., erosivity). Friction velocity is generally calculated from surface-wind fluctuations using high response sensors or from vertical profiles of time-averaged wind speed and air temperature assuming flux profile relationships within the surface boundary layer (i.e., the inertial sub-layer). When the surface is covered with vegetation, the total shear-stress term, T, is split into a pressure drag on the roughness elements, skin drag on the ground surface, and skin drag on the roughness element surface (Shao, 2008). For monitoring friction velocity of total shear stress, observation over the saltation layer is required because within the saltation layer part of the total shear stress is used for sand particle motion. This alters the wind profile within the saltation layer making application of standard boundary-layer relationships (i.e., "the law of the wall") highly uncertain (Bauer et al., 2004). For vertical wind-speed profile measurements, it is not necessary to monitor turbulent fluctuations of meteorological elements so sensors with lower time-response are sufficiently accurate. For surfaces with larger rough components, however, such as hilly regions and surfaces with vegetation, careful analyses are required for evaluation of roughness length, zero-plane displacement, and stability correction terms for individual profiles (Mikami et al., 1996). Ideally, multiple vertical profiles of wind speed are needed to characterize spatial variability of the wind field to estimate mean values for these aerodynamic parameters of interest (Raupach et al., 2006; King et al., 2008).

Soil physical parameters of interest include soil particle-size distributions for fully disturbed and minimally disturbed soils, soil crust strength, and soil moisture of the thin surface layer. Among these parameters, soil particle-size distribution data are key because this is an initial and restricted condition for particle-size distributions that will be transported by saltation and emitted as dust. Usually, soil particles are aggregated due to binding forces and cementing agents (e.g., salt bridges between particles), so there is considerable difference between soil particle-size distributions of minimally disturbed soil and its fully disturbed or disaggregated state. Measurement of these size distributions is often inconsistent due to different measurement principles associated with different particle-size analyzers. There is no measurement standard for determining soil particle-size distributions. This increases the difficulty of establishing a standardized global-scale database of soil particle-size distributions. Thus, future needs for improved soil particle size information include (1) soil samples at different depths (e.g., 1, 5, 10 mm etc.); (2) homogenization of particle size data derived from techniques of analysis; (3) establishment of an international soil standard specific for aeolian research, complementary to those already exists for soil physics and soil hydrology; and (4) extension of soil analysis to soil mineralogy and nutrients.

Parameters for specifying vegetation conditions include vegetation cover, frontal-area index (λ), leaf are index (LAI), NDVI, biomass of both living and dead vegetation, porosity, and size (height and breadth). For surfaces with dense vegetation cover, dust emission rarely occurs due to the protection the vegetation offers to the surface. When vegetation is sparsely distributed, it acts as roughness elements on the surface, which alter the roughness height, zero-plane displacement, and drag force as described in Section 3.

5.1.2. Monitoring of sand and dust fluxes

In concert with monitoring of wind speed for evaluating friction velocity and threshold-friction velocity, simultaneous monitoring of saltation and dust emission fluxes are required for understanding dust emission processes. In most dust emission schemes, saltation flux Q is a function of friction velocity and threshold friction velocity u_{*t}. The effect of soil and surface factors also is expressed by a weight function, f, that is multiplied by $u_{*t}(d_s)$, where d_s is sand-particle size. Dust emission flux, F, is usually expressed as a function of Q (Shao, 2008). Thus, in order to understand dust emission processes and validate a dust emission scheme, both Q and F must be monitored with higher time resolution than friction velocity. The mass fluxes of Q and F are primarily functions of sand and dust particle sizes, d_i and d_s, so that size-resolved monitoring of saltation and dust particles is needed.

Most conventional sensors of Q and F have limitations on time and/or particle size resolution (Shao, 2008). Recently, highly time-resolved measurements of saltation particle size and saltation activity have been made using the Sand Particle Counter (SPC; Mikami et al., 2005). The SPC was developed and used for field studies. It is currently configured to measure particle sizes in the range of 40 to 600 μm with 32 channels, covering the entire sand-particle size range. The SPC has a sampling rate of 1 Hz. Placing multiple SPC sensors within saltation layers, allows for estimation of horizontal sand flux Q assuming a quadratic exponential function of the form $q(z, d_S) = q_0 \exp(-az - bz^2)$ (Mikami et al., 2010).

For monitoring dust particle mass concentrations, high- and low-volume samplers are widely used for monitoring of Total Suspended Particulates (TSP) as well as two size fractions associated with air quality standards (i.e., the concentration of particles $\leqslant$10 μm and $\leqslant$2.5 μm aerodynamic diameters [i.e., PM_{10} and $PM_{2.5}$]). Time resolution of these sensors, however, usually ranges from several hours to several weeks. This is unsatisfactory for monitoring dust emission processes. Due to these long sampling times, the instruments are not relevant for understanding the physics of the dust emission process.

If dust particle sensors are set in an environment that satisfies a horizontally homogeneous condition the vertical dust flux can be evaluated by analogy with turbulent flux calculations for a scalar quantity such as applies to gases. In this case, vertical flux can be estimated by application of the gradient method, which requires vertical profiles of dust particle number concentrations for multiple particle sizes (Sow et al., 2009; Ishizuka et al., 2010). Eddy correlation techniques also are applicable but require measurement of the fluctuation of dust particle number concentrations at very high sampling rates (Fratini et al., 2007), which is difficult to achieve for dust-sized particles.

Optical particle counter (OPC) technology is a sensor capable of monitoring particle size and number concentrations at high time resolution (typically 1 Hz), although particle-size information from OPC sensors is sometimes unreliable, because OPC assumes the shape of dust particles to be spherical although they are typically non-spherical. Multiple OPC sensors arrayed vertically within the surface layer can be used to estimate vertical dust flux using the gradient method. Careful calibration of the OPC is required to ensure accuracy of the number concentration measurements.

Ishizuka et al. (2010) report observations of vertical dust concentrations using an OPC system in a fallow field in Australia as a part of the JADE project. The OPC used in that study counts the number of suspended dust particles in eight size bins 0.3–0.5, 0.5–0.7, 0.7–1, 1–2, 2–3, 3–5, 5–7, and >7 μm in diameter at 1 Hz. They found that temporal variations of dust concentration and dust flux are controlled by turbulent eddy motion, because particle-size dependencies for dust concentrations at different heights cannot be found in their observations. Using a conventional gradient method, Ishizuka et al. (2010) estimated the dust flux at their site and found three transport modes for the dust, which they related to changes in the relationship between u_* and Q. The first mode is called the saltation bombardment mode that occurs when

Please cite this article in press as: Shinoda, M., et al. Temperate grasslands as a dust source: Knowledge, uncertainties, and challenges. Aeolian Research (2011), doi:10.1016/j.aeolia.2011.07.001

saltation is significant and sustained ($u_* > u_{*t}$); the second mode is a transition mode that occurs when saltation is marginal and intermittent ($u_* \approx u_{*t}$). The third mode occurs when dust is present, but the wind is weak ($u_* < u_{*t}$). In case of the first mode, dust flux increases roughly with $u_*^{3\sim5}$. However in case of the third mode, flux does not obey the power law relation with u_* because, in this case, saltation bombardment is no longer the main mechanism for dust emission and the observed ambient dust is either due to advective dust or aerodynamic entrainment.

5.2. Monitoring of the processes over Northeastern Asia

It is well known that northeastern Asia is the world's second largest dust source region. Compared to the Saharan desert, distributions of vegetation cover and land use are complex in Asia and show clear seasonal change plus strong inter-annual variations (Zou and Zhai, 2004; Kurosaki and Mikami, 2005). Dust emission is primarily controlled by wind-generated shear stress (Kurosaki and Mikami, 2003; Lee and Sohn, 2009). In East Asia, however, land surface conditions are important secondary controlling factors (Kurosaki and Mikami, 2004). Many analytical studies have been done in Asia to discern the effects of ground surface conditions on dust outbreaks and emissions using SYNOP surface observation (Kurosaki and Mikami, 2005; Lee and Sohn, 2009) and satellite data (Kurosaki and Mikami, 2004; Zou and Zhai, 2004; Liu et al., 2004). Intensive observation of dust emission processes over sparse grasslands in this region is limited, however.

The increase in vegetation during the growing season may be an important factor preventing dust outbreaks in eastern Inner Mongolia (Lee and Sohn, 2009). Recent overcultivation and overgrazing within this region of Mongolia are likely affecting dust emissions. Thus, Mongolia is a dust source region sensitive to ground surface conditions especially vegetation. Timely monitoring is needed to evaluate Mongolia's susceptibility to soil degradation (i.e., erodibility) and the associated increase in emission potential.

Based on the premise that vegetation plays a critical role in dust emissions in TGs, the Dust-Vegetation Interaction Experiment (DUVEX) was initiated to develop a biogeophysical model that can simulate dust emission and ecosystem processes over these vegetated land surfaces (Shinoda et al., 2010a). The DUVEX project is also aimed at developing an understanding of interactions between dust emissions, ground surface conditions (e.g., vegetation distribution patterns), soil moisture, surface soil particle size distributions, and connections with anthropogenic effects caused by overgrazing.

The observation site for DUVEX is Bayan Unjuul (47.04°N, 105.95°E), north of the most frequent dust outbreak region in Mongolia. Mean annual precipitation at the site is 163 mm, and mean annual temperature is 0.1 °C. The site is located in central Mongolia, and this dust outbreak region is sensitive to variations in snow cover and vegetation (Kurosaki and Mikami, 2007). In addition, grazing in this area puts pressure on the vegetation to remain in a healthy and robust state. These factors (i.e., snow cover, vegetation conditions, and overgrazing) will affect dust emission at the site. Long-term monitoring of dust emission processes here will be important to our understanding of inter-annual and seasonal variations of dust emission in connection with ground surface conditions for this TG region.

The first DUVEX intensive observational period (IOP) was from 24 to 27 April 2008. During this IOP, simultaneously with the atmosphere and sand/dust monitoring observations, vegetation cover, NDVI using spectral irradiance (>3 nm), width of the remnant plant stand left after grazing, and soil sampling measurements were carried out to characterize land-surface conditions (Shinoda et al., 2010a).

During the first IOP, which was prior to the growing season, no green vegetation was observed, but some grazed vegetation with dead brown-colored leaves remained from the previous year. The topsoil was sandy and very dry. In the northwest part of the Dust Observing Site (DOS), vegetation cover and ground-observed NDVI were highly correlated ($r^2 = 0.93$). The vegetation cover and MODIS-estimated NDVI were 7.2% and 0.123, respectively, both satisfying conditions known to facilitate dust emission on the Loess Plateau of China (vegetation cover <18% and NDVI <0.2) (Kimura et al., 2009).

On 24 April, 2008, a weak dust storm occurred at the site; and the threshold wind speed for sand saltation movement measured at 1.54 m (AGL) was estimated to be 8.9 m s^{-1}. Although the vegetation cover was very low and grazed plant height was not high, the threshold wind speed at this vegetated site was substantially higher than typical of warm desert environments with low vegetation cover. These results suggest that if the vegetation produced in the previous summer season remains through the succeeding cold grazing season it may exert a carry-over effect on spring dust emissions. Such an effect was observed for this site by Shinoda et al. (2010b) and for the other arid regions by several ecological studies (Haddad et al., 2002; Lauenroth and Sala, 1992; Oesterheld et al., 2001; Wiegand et al., 2004).

Recently, from insight obtained in the DUVEX campaign, the positive effect of dry dead leaves on dust emission is being monitored with considerable interest. Kurosaki et al. (2011a) analyzed SYNOP data over East Asia to understand the relation between dust outbreak and ground-surface condition. They showed that dust outbreak frequency increased while frequency of strong wind, which is a wind whose speed exceeds 5-percentile of threshold wind speeds for 1970–2009, decreased or changed little from the 1990s to 2000s in Mongolia, eastern Inner Mongolia, and northeastern China. 5-percentile of threshold wind speed decreased in these sub-regions over the period, and this suggests that ground-surface condition changed more vulnerable for dust outbreak, resulted in the increase of dust outbreak frequency. Precipitation amount for June to August (i.e., vegetation growing season) and annual maximum NDVI decreased in some areas of Mongolian grassland during the period noted. These results suggest that decreased precipitation causes a reduction in vegetation amount in a summer. This decreases the amount of dead-brown leaves in spring in the following year, and enhances dust emission due to loss of protective cover. These hypothesized processes are referred to as the dead-leaf hypothesis (Kurosaki et al, 2011a,b).

There is also a relationship between maximum NDVI in the previous year and the dead-brown leaves NDVI in the next spring season (Fig. 13). Dead-brown leaves and living green leaves have different reflectances in the near-infrared (NIR; 0.725–1.1 μm) and red range (RED; 0.55–0.68 μm). It is then theoretically possible to evaluate the difference in relative amounts of brown and green leaves from the NIR and RED reflectance signals using satellite remote sensing data such as AVHRR. Consideration and monitoring of seasonal change of spectral reflectance from summer season to the coming spring season are required.

Kimura and Shinoda (2010) modeled spatial distribution of threshold wind speeds for dust events in northeast Asia using their observations at a Mongolian station. Using a map of NDVI, they estimated spatial distributions of vegetation cover, roughness length, threshold friction velocity, and threshold wind speed. They showed it was possible to predict the threshold wind speed in the next dust season using maximum NDVI from the previous year. Although the NDVI was initially developed as an indicator of greenness of vegetation or land surface, Kimura and Shinoda (2010) showed that ground-based NDVI measurements can be used as an indicator of vegetation cover up to 20% even when the vegetation is composed of dead materials. Thus, satellite-derived NDVI holds the promise to extend this method to a wider area including

Please cite this article in press as: Shinoda, M., et al. Temperate grasslands as a dust source: Knowledge, uncertainties, and challenges. Aeolian Research (2011), doi:10.1016/j.aeolia.2011.07.001

the ability to account for sparse brown vegetation (dead leaves), which is commonly observed during the pre-growth spring season in grassland regions.

5.3. Monitoring needs

In future field experiments, an explicit focus should be placed on an integrated approach that combines measurements of vegetation structure, dynamics, and physiology with measurements of aeolian processes. In general, vegetation structure parameters include height; density; size; and spatial distribution of trees, shrubs and herbs as well as standing biomass such as various aboveground fractions (e.g., wood, leaves, and reproductive structures) and belowground fractions (coarse and fine roots).

Recent improvements in instruments for measuring saltation and dust emission processes have enabled more precise monitoring of particle size with increased time resolution (Mikami et al., 2010; Ishizuka et al., 2010). When particle size distribution data are combined with simultaneous observation of friction velocity, validation of wind erosion models can be advanced. Knowledge of the spectrum of particle sizes in suspension and their associated vertical gradients is critical for proper measurement of the total flux (Shao et al., 2011).

Progress in characterization and monitoring of vegetation has been less well-developed as it relates to wind erosion. As we have shown, living-green or dead-brown leaves can have considerable effect on the dust emission process. To monitor both vegetation characteristics over semiarid sparsely vegetated regions will require use of remote sensing data. One approach has been to use NDVI data obtained by AVHRR (resolution of 1 km) or LandSat TM image (resolution of 30 m). Their signals contain a mixture of vegetation and amounts of living and dead biomass as well as information on soils. The range of remotely sensed NDVI changes from 0.8 for dense vegetation to about 0.3 to 0.12 for dead leaves and dry soil. Thus, it is still difficult to separate vegetation information from living (green) to dead (brown). There is a difference, however, in spectral reflectance properties between green and brown vegetation. A real-time monitoring of reflectivity with wavelength from 0.4 to 1.1 μm would be useful for qualitative evaluations of vegetation indices for these two conditions (i.e., green-living/brown-dead).

According to Shao (2008), for wind erosion and dust emission modeling, land-surface parameters can be classified into the following three categories:

- Soil properties such as soil texture, soil-salt content, soil-binding strength, etc.
- Surface aerodynamic properties such as frontal area index, erodible fraction, roughness length, etc.
- Soil thermal and hydraulic properties required by land-surface modeling.

Most of these properties, however, are not found within a comprehensive global scale database. Although some institutions (e.g., FAO, ISRIC and USDA) already developed global soil databases, they are mostly limited to soil types, horizons etc. and do not contain the attributes and parameters required for wind erosion modeling. The particle size classifications for the different soil types are insufficiently detailed, e.g., soils classified as loam may have substantially different particle size characteristics. The databases for other parameters are also rather incomplete, such as aerodynamic roughness length and fraction of roughness-elements cover. To more accurately represent direct and indirect aerosol radiative perturbations that are caused by mineral dust particles arising from wind erosion, it will be necessary to develop a robust dust-emission model that effectively predicts the spectrum of particle sizes. For this to proceed, it will also be necessary to construct a global data set of soil properties. This is an issue of some urgency as it will be necessary to combine the model with soils data to advance wind erosion research and increase our understanding of the impact of dust on climate.

6. Concluding remarks

In this review paper, we summarized state-of-the-art understanding of TG wind-erosion processes and identified uncertainties and research needs. We also outlined the DUVEX project that has as its main goal further development of the TG wind-erosion modeling system.

A deeper understanding of the aerodynamic and physical controls of grassland vegetation on wind erosion and dust emission processes remains a challenge. Additionally, much of what is known has arisen from small-scale wind tunnel and limited field testing. Scaling known relationships upwards to model the regional scale remains to be evaluated. This applies to both models for entrainment and transport of sediments as well as aerodynamics of vegetated surfaces. Validation of surface characterization measurements obtained via remote-sensing techniques and their relationship with surface and aerodynamic roughness remains to be undertaken, but these techniques hold promise as a means to quantify critical parameters affecting dust emissions that cannot be obtained for large regions by other means.

Integrated wind-erosion modeling systems that couple models of atmospheric, land-surface, and aeolian processes with dust observations and land-surface parameter databases are available. In these models, land-surface conditions, soil texture, soil moisture, vegetation cover, and roughness elements have been taken into consideration, but with varying degrees of sophistication. These parameters differ in time and are spatially heterogeneous, and their specifications with accuracy have proven to be difficult. The following tasks stand out as key issues we must tackle in the next stage of model development: (1) establishment of grassland aeolian database including soil physical properties, (2) size-resolved monitoring of sand and dust fluxes over TGs, (3) near real-time monitoring of land-surface conditions over TGs, (4) grassland vegetation model that simulates both vegetation growth and decay plus the impact of grazing as observed at the DUVEX site representative of a typical steppe, (5) coupling the vegetation model with a wind-erosion model, and (6) data assimilation using satellite and Lidar data, with a focus on soil moisture and vegetation.

Once such modeling systems are established, they will have practical applications in the following: (1) hazard mapping of severe dust storms, (2) guidelines for optimum spatial allocation of livestock to avoid wind erosion due to overgrazing, and (3) guidelines for rehabilitation of degraded grasslands due to wind erosion.

Acknowledgements

We would like to thank Dr. B. Nandintsetseg for her support in preparing this manuscript. This review paper was based on the discussion made at the International Symposium on Dust-Vegetation Interaction on 27 February 2010 that was funded by the Invitation Program for Advanced Research Institutions in Japan of the Japan Society for the Promotion of Science.

References

Alfaro, S.C., Gomes, L., 2001. Modeling mineral aerosol production by wind erosion: Emission intensities and aerosol size distribution in source areas. J. Geophys. Res. 106, 18075–18084.

Archibold, O.W., 1995. Ecology of World Vegetation. Chapman & Hall, London.

Barnes, R.F., Beard, J.B. (Eds.) 1992. Glossary of Crop Science Terms. Crop Science Society of America, Madison, p. 88.

Bauer, S.E., Balkanski, Y., Schulz, M., Hauglustaine, D. A., Dentener, F., 2004. Global modeling of heterogeneous chemistry on mineral aerosol surfaces: influence on tropospheric ozone chemistry and comparison to observations. J. Geophys. Res. Atmos. 109. doi:10.1029/2003JD003868.

Belnap, J., Gillette, D.A., 1997. Disturbance of biological soil crusts: impacts on potential wind erodibility of sandy desert soils in SE Utah. Land Deg. Dev. 8, 355–362.

Bilbro, J.D., Fryrear, D.W., 1994. Wind erosion losses as related to plant silhouette and soil cover. Agron. J. 86, 550–553.

Binkowski, F.S., Shankar, U., 1995. The regional particulate model 1. Model description and preliminary results. J. Geophys. Res. 100 (D12), 26191–26209.

Bou Karam, D., Flamant, C., Tulet, P., Chaboureau, J.-P., Dabas, A., Todd, M.C., 2009. Estimate of Sahelian dust emissions in the intertropical discontinuity region of the West African Monsoon. J. Geophys. Res. 114, D13106. doi:10.1029/2008JD011444.

Buckerly, R., 1987. The effect of sparse vegetation in the transport of sand dune by wind. Nature 325, 426–428.

Bullock, M.S., Larnet, F.J., Cesar Izaurralde, R., Feng, Y., 2001. Over winter changes in wind erodibility of clayloam soils in southern Alberta. J. Soil Sci. Soc. Am. 65, 423–430.

Cavazos, C., Todd, M.C., Schepanski, K., 2009. Numerical model simulation of the Saharan dust event of 6–11 March 2006 using the Regional Climate Model version 3 (RegCM3). J. Geophys. Res. 114, D12109. doi:10.1029/2008JD011078.

Chappell, A., Van Pelt, S., Zobeck, T., Dong, Z., 2010. Estimating aerodynamic resistance of rough surfaces using angular reflectance. Rem. Sens. Environ. 114, 1462–1470.

Chepil, W.S., 1944. Utilization of crop residues for wind erosion control. Sci. Agr. 24 (7), 307–319.

Chimgee, D., Shinoda, M., Tachiiri, K., Kurosaki, Y., 2010. Why did a synoptic storm cause a dramatic damage in a limited area of Mongolia? Mongolian Population J. 19, 63–68.

Chun, H.Y., Song, M.D., Kim, J.W., Baik, J.J., 2001. Effects of gravity wave drag induced by cumulus convection on the atmospheric general circulation. J. Atmos. Sci. 58, 302–319.

Coffin, D.P., Lauenroth, W.K., 1989. Disturbances and gap dynamics in a semiarid grassland: a landscape-level approach. Landsc. Ecol. 3, 19–27.

Cooke, R., Warren, A., Goudie, A., 1993. Desert Geomorphology. UCL Press, London, 526 p.

Counihan, J., 1971. Wind tunnel determination of the roughness length as a function of the fetch and the roughness density of three-dimensional roughness elements. Atmos. Environ. 5, 637–642.

Crosson, W.L., Laymon, C.A., Inguva, R., Schamschula, M.P., 2002. Assimilating remote sensing data in a surface flux-soil moisture model. Hydrol. Proc. 16, 1645–1662.

Crow, W.T., Wood, E.F., 2003. The assimilation of remotely sensed soil brightness temperature imagery into a land surface model using Ensemble Kalman filtering: a case study based on ESTAR measurements during SGP97. Adv. Water Resour. 26, 137–149.

Dickinson, R.E., Henderson-Sellers, A., Kennedy, P.J., 1993. Biosphere-Atmosphere Transfer Scheme (BATS) Version le as coupled with the NCAR Community Land Model, NCAR, Technical Note TN383+STR, 72 pp.

Dong, J., Kaufmann, R.K., Myneni, R.B., Tucker, C.J., Kauppi, P.E., Liski, J., Buermann, W., Alexeyev, V., Hughes, M.K., 2003. Remote sensing estimates of boreal and temperate forest woody biomass, carbon pools, sources and sinks. Rem. Sens. Environ. 84, 393–410.

Elliot, W.P., 1958. The growth of the atmospheric internal boundary layer. Am. Geophys. Union. Trans. 39, 1048–1054.

Etyemezian, V., Nikolich, G., Ahonen, S., Pitchford, M., Sweeney, M., Purcell, R., Gillies, J., Kuhns, H., 2007. The portable in situ wind erosion laboratory (PI-SWERL): a new method to measure PM_{10} windblown dust properties and potential for emissions. Atmos. Environ. 41, 3789–3796.

Fécan, F., Marticorena, B., Bergametti, G., 1999. Parameterization of the increase of the aeolian erosion threshold wind friction velocity due to soil moisture for arid and semiarid areas. Ann. Geophys. 17, 149–157.

Fratini, G., Ciccioli, P., Febo, A., Forgione, A., Valentini, R., 2007. Size-segregated fluxes of mineral dust from a desert area of northern China by eddy covariance. Atmos. Chem. Phys. 7, 2839–2854.

Fryrear, D.W., 1985. Soil cover and wind erosion. Trans. Am. Soc. Agric. Eng. 28, 781–784.

Genthon, C., 1992. Simulations of desert dust and sea salt aerosols in Antarctica with a general circulation model of the atmosphere. Tellus B 44, 371–389.

Gillette, D.A., 1988. Threshold friction velocities for dust production for agricultural soils. J. Geophys. Res. 93, 12645–12662.

Gillette, D.A., Ono, D., 2008. Expressing sand supply limitation using a modified Owen saltation equation. Earth. Surf. Proc. Land. 33, 1806–1813.

Gillette, D.A., Stockton, P.H., 1989. The effect of nonerodible particles on the wind erosion of erodible surfaces. J. Geophys. Res. 94, 12885–12893.

Gillette, D.A., Passi, R., 1988. Modeling dust emission caused by wind erosion. Journal of Geophysical Research 93 (11), 14234–14242.

Gillette, D.A., Adams, J., Endo, E., Smith, D., 1980. Threshold velocities for input of soil particles into the air by desert soils. J. Geophys. Res. 85, 5621–5630.

Gillette, D.A., Fryrear, D.W., Gill, T.E., Ley, T., Cahill, T.A., Gearhart, E.A., 1997. Relation of vertical flux of particles smaller than 10 μm to total aeolian horizontal mass flux at Owen Lake. J. Geophys. Res. 102, 26009–26015.

Gillies, J.A., Lancaster, N., Nickling, W.G., Crawley, D.M., 2000. Field determination of drag forces and shear stress partitioning effects for a desert shrub (*Sarcobatus vermiculatus*, greasewood). J. Geophys. Res. 105, 24871–24880.

Gillies, J.A., Nickling, W.G., King, J., 2002. Drag coefficient and plant form response to wind speed in three plant species: Burning Bush (*Euonymus alatus*), Colorado Blue Spruce (*Picea pungens glauca*), and Fountain Grass (*Pennisetum setaceum*). J. Geophys. Res. 107, 4760. doi:10.1029/2001JD001259.

Gillette, D.A., Herrick, J., Herbert, G.A., 2006. Wind characteristics of mesquite streets in the northern Chihuahuan Desert, New Mexico, USA. Environ. Fluid Mech. 6, 241–275.

Gillies, J.A., Nickling, W.G., King, J. 2006. Aeolian sediment transport through large patches of roughness in the atmospheric inertial sublayer. J. Geophys. Res. Earth Surf. 111. doi:10.1029/2005JF000434.

Gillies, J.A., Nickling, W.G., King, J., 2007. Shear stress partitioning in large patches of roughness in the atmospheric inertial sublayer, Bound. Layer Meteorol. 122 (2), 367–396.

Gillies, J.A., Nickling, W.G., Lancaster, N., 2010. Vegetative roughness controls on wind erosion: a shear stress partitioning approach. In: Saxena, M. (Ed.), Ninth International Conference on Dryland Development: Sustainable Development in the Drylands - Meeting the Challenge of Global Climate Change, Alexandria, Egypt.

Ginoux, P., Prospero, J.M., Torres, O., Chin, M., 2004. Long-term simulation of global dust distribution with the GOCART model: correlation with North Atlantic Oscillation. Environ. Model. Soft. 19, 113–128.

Grant, P.F., Nickling, W.G., 1998. Direct field measurement of wind drag on vegetation for application to windbreak design and modeling. Land Degrad. Develop. 9, 57–66.

Gregorich, E.G., Greer, K.J., Anderson, D.W., Liang, B.C., 1998. Carbon distribution and losses: erosion and deposition effects. Soil Tillage Res. 47, 291–302.

Haddad, N.M., Tilman, D., Knops, J.M.H., 2002. Long-term oscillations in grassland productivity induced by drought. Ecol. Lett. 5, 110–120.

Hagen, L.J., 1991. Wind erosion mechanics: abrasion of aggregated soil. Trans. Am. Soc. Agric. Eng. 34, 831–837.

Hagen, L.J., Wagner, L.E., Tatarko, J., 1996a. Wind Erosion Prediction System. Technical Documentation, USDA.

Hagen, L.J., Mirzomostafa, N., Hawkins, A., 1996b. PM-10 generation by wind erosion. Proc. Int.Conf. on Air Pollution from Agricultural Operations. Kansas City, MO, pp. 79–86.

Hall, D.J., Macdonald, R., Walker, S., Spanton, A.M., 1996. Measurements of dispersion within simulated urban arrays – a small scale wind tunnel study. Report, BRE Client Report CR 178/96, Garston Watford.

Hatfield, J.L., 1989. Aerodynamic properties of partial canopies. Forest. Meteorol. 46, 15–22.

Heinold, B., Tegen, I., Schepanski, K., Hellmuth, O., 2008. Dust radiative feedback on Saharan boundary layer dynamics and dust mobilization. Geophys. Res. Letteres 35, L20817. doi:10.1029/2008GL035319.

Hoffmann, C., Funk, R., Wieland, R., Li, Y., Sommer, M., 2008a. Effects of grazing and topography on dust flux and deposition in the Xilingele grassland, Inner Mongolia. J. Arid. Environ. 72, 792–807.

Hoffmann, C., Funk, R., Li, Y., Sommer, M., 2008b. Effect of grazing on wind driven carbon and nitrogen ratios in the grasslands of Inner Mongolia. Catena 75, 182–190.

Husar, R.B., Tratt, D.M., Schichtel, B.A., Falke, S.R., Li, F., Jaffe, D., Gassó, S., Gill, E., Laulainen, N.S., Lu, F., Reheis, M.C., Chun, Y., Westphal, D., Holben, B.N., Gueymard, C., McKendry, I., Kuring, N., Feldman, G.C., McClain, C., Frouin, R.J., Merril, J., DuBois, D., Vignola, F., Murayama, T., Nickovic, S., Wilson, W.E., Sassen, K., Sugimoto, N., Malm, W.C., 2001. Asian dust events of April 1998. J. Geophys. Res. 106, 18317–18330.

IPCC WG I (Intergovernmental Panel on Climate Change Working Group I), 2007. Climate Change 2007: The Physical Science Basis. Cambridge: Cambridge University Press, p. 800.

Ishizuka, M., Mikami, M., Yamada, Y., Zeng, F., Gao, W., 2005. An observational study of soil moisture effects on wind erosion at a gobi site in the Taklimakan desert. J. Geophys. Res. 110, D18S03. doi:10.1029/2004JD004709.

Ishizuka, M., Mikami, M., Leys, J., Yamada, Y., Heidenreich, S., Shao, Y., McRanish, G.H., 2008. Effects of soil moisture and dried raindroplet crust on saltation and dust emission, J. Geophys. Res. 113. doi:10.1029/2008JD009955.

Ishizuka, M., Mikami, M., Shao, Y., Leys, J.F., Yamada, Y., Heidenreich, S., 2010. Dust flux measurements at a fallow wheat field using optical particle counter. In: Proceedings of 7th International Conference on Aeolian Research.

Jackson, P.S., 1981. On the displacement height in the logarithmic velocity profile. Journal of Fluid Mechanics 111, 15–25.

Kimura, R., Shinoda, M., 2010. Spatial distribution of threshold wind speeds for dust outbreaks in northeast Asia. Geomorphology 119, 315–329.

Kimura, R., Bai, L., Wang, J., 2009. Relationships among dust outbreaks, vegetation cover, and surface soil water content on the Loess Plateau of China, 1999–2000. Catena 77, 292–296.

King, J., Nickling, W.G., Gillies, J.A., 2005. Representation of vegetation and other non-erodible elements in aeolian sediment transport models. J. Geophys. Res. Earth Surf. 110, F04015. doi:10.1029/2004JF000281.

King, J., Nickling, W.G., Gillies, J.A., 2008. Investigations the law-of-the-wall over sparse roughness elements. J. Geophys. Res. Earth-Surf. 113, F02S07. doi:10.1029/2007JF000804.

Please cite this article in press as: Shinoda, M., et al. Temperate grasslands as a dust source: Knowledge, uncertainties, and challenges. Aeolian Research (2011), doi:10.1016/j.aeolia.2011.07.001

Kurosaki, Y., Mikami, M., 2003. Recent frequent dust events and their relation to surface wind in East Asia, Geophys. Res. Lett. 30(14), 1736. doi:10.1029/2003GL017261.

Kurosaki, Y., Mikami, M., 2004. Effect of snow cover on threshold wind velocity of dust outbreak, Geophys. Res. Lett. 31, L03106. doi:10.1029/2003GL018632.

Kurosaki, Y., Mikami, M., 2005. Regional difference in the characteristic of dust event in East Asia: relationship among dust outbreak, surface wind, and land surface condition. J. Met. Soc. Japan 83A, 1–18.

Kurosaki, Y., Mikami, M., 2007. Threshold wind speed for dust emission in east Asia and its seasonal variations, J. Geophys. Res. 112, D17202. doi:10.1029/2006JD007988.

Kurosaki, Y., Shinoda, M., Mikami, M., 2011a. What caused a recent increase in dust outbreaks over East Asia? Geophys. Res. Lett. 38, L11702. doi:10.1029/2011GL047494.

Kurosaki, Y., Shinoda, M., Mikami, M., Nandintsetseg, B., 2011b. Effects of soil and land surface conditions in summer on dust outbreaks in the following spring in a Mongolian grassland. SOLA 7, 69–72.

Lancaster, N., Baas, A., 1998. Influence of vegetation cover on sand transport by wind: Field studies at Owens Lake. California Earth. Surf. Proc. Land. 23, 69–82.

Lauenroth, W.K., Sala, O.E., 1992. Long-term forage production of North American shortgrass steppe. Ecol. Appl. 2, 397–403.

Lee, E.-H., Sohn, B.-J., 2009. Examining the impact of wind and surface vegetation on the Asian dust occurrence over three classified source regions, J. Geophys. Res. 114, D06205. doi:10.1029/2008JD010687.

Lepers, E., Lambin, E.F., Janetos, A.C., DeFries, R., Achard, F., Ramankutty, N., Scholes, R.J., 2005. A synthesis of rapid land-cover change information for the 1981–2000 period. Bioscience 55 (2), 115–124.

Lettau, H.H., 1969. Note on aerodynamic roughness-parameter estimation on the basis of roughness element description. J. Appl. Meteor. 8, 828–832.

Leys, J.F., 1991. Towards a better model of the effect of prostrate vegetation cover on wind erosion. Vegetation 91, 49–58.

Leys, J., McTainsh, G., Strong, C., Heidenreich, S., Biseaga, K., 2008. Dust Watch: community networks to improve wind erosion monitoring in Australia. Earth Surf. Proc. Landforms 33, 1912–1926.

Li, J., Okin, G.S., Alvarez, L., Epstein, H., 2007. Quantitative effects of vegetation cover on wind erosion and soil nutrient loss in a desert grassland of southern New Mexico, USA. Biogeochemistry 85, 317–332.

Li, R., Min, Q.L., Harrison, L.C., 2010. A case study: the indirect aerosol effects of mineral dust on warm clouds. J. Atmos. Sci. 67, 805–816.

Liedtke, J., 1992. An experimental investigation into the dispersion behavior in neutral and unstable zero pressure gradient boundary layers with different roughnesses. Ph.D. thesis, University of Bundeswehr, Munich.

Liu, L.Y., Shi, P.J., Zou, X.Y., Gao, S.Y., Erdon, H., Yan, P., Li, X.Y., Dong, Z.B., Wang, J.H., 2003. Short-term dynamics of wind erosion of three newly cultivated grassland soils in Northern China. Geoderma 115, 55–64.

Liu, X., Yin, Z.-Y., Zhang, X., Yang, X., 2004. Analyses of the spring dust storm frequency of northern China in relation to antecedent and concurrent wind, precipitation, vegetation, and soil moisture conditions. J. Geophys. Res. 109, D16210. doi:10.1029/2004JD004615.

Liu, Z.F., Liu, G.H., Fu, B.J., Zheng, X.Q., 2008. Relationship between plant species diversity and soil microbial functional diversity along a longitudinal gradient in temperate grasslands of Hulunbeir, Inner Mongolia, China. Ecol. Res. 23, 511–518.

Los, S.O., Collatz, G.J., Bounoua, L., Sellers, P.J., Tucker, C.J., 2001. Global interannual variations in sea surface temperature and land surface vegetation, air temperature, and precipitation. J. Clim. 14, 1535–1549.

Lyles, L., Allison, b.E., 1976. Wind erosion: the protective role of simulated standing stubble. Trans. Am. Soc. Agric. Engrs. 19, 61–64.

Lyles, L., Allison, B.E., 1981. Equivalent wind-erosion protection from selected crop residues. Trans. ASAE 24, 405–408.

Lyles, L., Schrandt, R.L., Schmeidler, N.F., 1974. Commercial soil stabilizers for temporary wind erosion control. Trans. ASAE 17, 1015–1019.

Macdonald, R.W., Griffiths, R.F., Hall, D.J., 1998. An improved method for the estimation of surface roughness of obstacle arrays. Atmos. Environ. 32, 3845–3862.

Macpherson, T., Nickling, W.G., Gillies, J.A., Etyemezian, V., 2008. Dust emissions from undisturbed and disturbed supply limited desert surfaces. J. Geophys. Res. Earth Surf. 113.

Mahowald, N.M., Kloster, S., Engelstaedter, S., Moore, J.K., Mukhopadhyay, S., McConnell, J.R., Albani, S., Doney, S.C., Bhattacharya, A., Curran, M.A.J., Flanner, M.G., Hoffman, F.M., Lawrence, D.M., Lindsay, K., Mayewski, P.A., Neff, J., Rothenberg, D., Thomas, E., Thornton, P.E., Zender, C.S., 2010. Observed 20th century desert dust variability: impact on climate and biogeochemistry. ACP 10, 10875–10893.

Mainguet, M., 1999. Aridity: Droughts and Human Development. Springer, Berlin, p. 302.

Mandakh, N., Dash, D., Khaulenbek, A., 2007. In: Tsogtbaatar, J. (Eds), Present Status of Desertification in Mongolia-Geoecological Issues in Mongolia. UB, pp. 63–73.

Marshall, J.K., 1971. Drag measurements in roughness arrays of varying density and distribution. Agric. Meteorol. 8, 269–292.

Marticorena, B., Bergametti, G., 1995. Modeling the atmospheric dust cycle: 1-design of a soil derived dust production scheme. J. Geophys. Res. 100, 16,415–16,430.

Marticorena, B., Bergametti, G., 1996. Two-year simulations of seasonal and interannual changes of the Sahran dust emission. Geophys. Res. Lett. 23 (15), 1921–1924.

Marticorena, B., Bergametti, G., Aumont, B., Callot, Y., N'Doume, C., Legrand, M., 1997. Modeling the atmospheric dust cycle: 2. Simulation of Saharan dust sources. J. Geophys. Res. 102D (4), 4387–4404.

Marticorena, B., Chazette, P., Bergametti, G., Dulac, F., Legrand, M., 2004. Mapping the aerodynamic roughness length of desert surfaces from the polder/adeos bidirectional reflectance product. Int. J. Rem. Sens. 25, 603–626.

Marticorena, B., Chatenet, B., Rajot, J.L., Traore, S., Coulibaly, M., Diallo, D., Kone, I., Maman, A., NDiaye, T., Zakou, A., 2010. Temporal variability of mineral dust concentrations over West Africa: Analyses of a pluriannual monitoring from the AMMA Sahelian Dust Transect. Atmos. Chem. Phys. 10, 8899–8915.

Mei, L., Wang, Z.Q., Cheng, Y.H., Guo, D.L., 2004. A review: factors influencing fine root longevity in forest ecosystem. Acta Phytoecologica Sinica 28 (5), 704–710 (in Chinese).

Menut, L., Masson, O., Bessagnet, B., 2009. Contribution of Saharan dust on radionuclide aerosol activity levels in Europe? The 21–22 February 2004 case study. J. Geophys. Res. 15 114, D16202. doi:10.1029/2009JD011767.

Middleton, N.J., 1991. Dust storms in the Mongolian People's Republic. Journal of Arid Environment 20, 287–297.

Mikami, M., Toya, T., Yasuda, N., 1996. An analytical method for the determination of the roughness parameters over complex regions. Bound. Layer. Met. 79, 23–33.

Mikami, M., Yamada, Y., Ishizuka, M., Ishimaru, T., Gao, W., Zeng, F., 2005. Measurement of saltation process over gobi and sand dunes in the Taklimakan desert, China, with newly developed sand particle counter, J. Geophys. Res. 110, D18S02. doi:10.1029/2004JD004688.

Mikami, M., Ishizuka, M., Shao, Y., Leys, J.F., Yamada, Y., Heidenreich, S., 2010. Total saltation flux estimated from time and size resolved measurements in JADE-IOP. In: Proceedings of 7th International Conference on Aeolian Research.

Mildred, C., 1984. The Gobi Desert. Virago, London.

Morinaga, Y., Tian, S., Shinoda, M., 2003. Winter snow anomaly and atmospheric circulation in Mongolia. Int. J. Climatol. 23, 1627–1636.

Moulin, S., Kergoat, L., Viovy, N., Dedieu, G., 1997. Global scale assessment of vegetation phenology using NOAA/AVHRR satellite measurements. J. Climat. 10, 1154–1170.

Musick, H.B., 1999. Field monitoring of vegetation characteristics related to surface changes in the Yuma Desert, Arizona and at the Jornada Experimental Range in the Chihuahuan Desert New Mexico. In: Breed, C.S., Reheis, M.C. (Eds.), Desert Winds: Monitoring Wind-Related Surface Processes in Arizona, New Mexico, California, U.S. Geological Survey Professional Paper 1589. US Government Printing Office, Washington, DC, pp. 71–84.

Musick, H.B., Trujillo, S.M., Truman, C.R., 1996. Wind-tunnel modelling of the influence of vegetation structure on saltation threshold. Earth. Surf. Proc. Land. 21, 589–605.

Musick, H.K., Gillette, D.A., 1990. Field evaluation of relationship between a vegetation structural parameter and sheltering against wind erosion, Land Degrad. Rehabilitation 2, 87–94.

Nandintsetseg, B., Shinoda, M., 2010. Seasonal change of soil moisture in Mongolia: Its climatology and modelling. Int. J. Climatol. doi:10.1002/joc.2134.

Natsagdorj, L., Jugder, D., Chung, Y.S., 2003. Analysis of dust storms observed in Mongolia during 1937–1999. Atmos. Environ. 37, 1401–1411.

Nickling, W.G., Gillies, J.A., 1989. Emission of fine-grained particulates from desert soils. In: Leinen, M., Sarnthein, M. (Eds.), "Paleoclimatology and Paleometeorology: Modern and Past Patterns of Global Atmospheric Transport" Series C Mathematical and Physical Sciences. Kluwer Academic Publishers, pp. 133–165.

Nickling, W.G., Gillies, J.A., 1993. Dust emission and transport in Mali, West Africa. Sedimentology 40, 859–868.

Nickling, W.G., McKenna Neuman, C., 1995. Development of deflation lag surfaces. Sedimentology 42, 403–414.

Nickovic, S., Dobricic, S., 1996. A model for long-range transport of desert dust. Mon. Wea. Rev. 124, 2537–2544.

Nickling, W.G., McTainsh, G.H., Leys, J.F., 1999. Dust emissions from the Channel Country of western Queensland, Australia. Z. Geomorph. N. F. 116, 1–17.

O'Loughlin, E.M., MacDonald, E.G., 1964. Some roughness-concentration effects on boundary resistance. La Houille Blanche 7, 773–782.

Oesterheld, M., Loreti, J., Semmartin, M., Sala, O.E., 2001. Inter-annual variation in primary production of a semi-arid grassland related to previous-year production. J. Veg. Sci. 12, 137–142.

Okin, G.S., 2005. Dependence of wind erosion and dust emission on surface heterogeneity: stochastic modeling. J. Geophys. Res. 110. doi:10.1029/2004JD005288.

Orndorff, R., 1998. A stochastic model of wind-induced shear stress partitioning between an erodible soil surface and roughness elements. In: Busacca, A.J. (Ed.), "Dust Aerosols, Loess Soils, Global Changes". Washington State University College of Agriculture and Home Economics, Pullman, WA, pp. 75–78.

Owen, R.P., 1964. Saltation of uniform grains in air. J. Fluid. Mech. 20, 225–242.

Pan, M., Wood, E.F., 2006. Data assimilation for estimating the terrestrial water budget using a constrained ensemble Kalman filter. J. Hydromet. 7, 534–547.

Parada, L.M., Liang, X., 2008. Impacts of spatial resolutions and data quality on soil moisture data assimilation. J. Geophys. Res. 113, D10101. doi:10.1029/2007JD009037.

Paruelo, J.M., Epstein, H.E., Lauenroth, W.K., Burke, I.C., 1997. ANPP estimates from NDVI for the Central Grassland Region of the United States. Ecology 78, 953–958.

Pérez, C., Nickovic, J., Baldasano, J.M., Sicard, M., Rochadenbosch, F., Cachorro, V.E., 2006. A long Saharan dust event over the western Mediterranean: lidar,

Sunphotometer observations, and regional dust modeling. J. Geophys. Res. 111, D15214. doi:10.1029/2005JD006579.
Peters, D.P.C., 2002. Recruitment potential of two perennial grasses with different growth forms at a semiarid transition zone. Am. J. Bot. 89, 1616–1623.
Piao, S.L., Mohammat, A., Fang, J.Y., Cai, Q., Feng, J.M., 2006. NDVI-based increase in growth of temperate grasslands and its responses to climate changes in China. Glob. Environ. Change 16, 340–348.
Pilinis, C., Seinfeld, J.H., 1987. Continued development of a general equilibrium model for inorganic multicomponent atmospheric aerosols. Atmos. Environ. 21, 2453–2466.
Priestley, C.H.B., 1959. Turbulent Transfer in the Lower Atmosphere. University of Chicago Press, p. 130.
Prospero, J.M., Ginoux, P. Torres, O., Nicholson, S.E., Gill, T.E., 2002. Environmental characterization of global sources of atmospheric soil dust identified with the NIMBUS 7 Total Ozone Mapping Spectrometer (TOMS) absorbing aerosol product. Review. Geophys. 40(1), 1002. doi:10.1029/2000RG000095.
Qian, W.H., Quan, L., Shi, S., 2002. Variations of the dust storm in China and its climatic control. J. Clim. 15, 1216–1229.
Raupach, M.R., 1992. Drag and drag partition on rough surfaces. Bound. Layer Meteorol. 60, 375–395.
Raupach, M.R., Thom, A.S., Edwards, I., 1980. A wind-tunnel study of turbulent flow close to regularly arrayed rough surfaces. Bound. Layer Meteorol. 18, 373–397.
Raupach, M.R., Gillette, D.A., Leys, J.F., 1993. The effect of roughness elements on wind erosion threshold. J. Geophys. Res. 98, 3023–3029.
Raupach, M.R., Hughes, D.E., Cleugh, H.A., 2006. Momentum absorption in rough-wall boundary layers with sparse roughness elements in random and clustered distributions. Bound.-Layer Meteorol. 120, 201–218. doi:10.1007/s10546-006-9058.
Reichle, R.H., McLaughlin, D.B., Entekhabi, D., 2002. Hydrologic data assimilation with the ensemble Kalman filter. Mon. Weather Rev. 130, 103–130.
Reinfried, F., Tegen, I., Heinold, B., Hellmuth, O., Schepanski, K., Cubasch, U., Huebener, H., Knippertz, P., 2009. Simulations of convectively-driven density currents in the Atlas region using a regional model: impacts on dust emission and sensitivity to horizontal resolution and convection schemes. J. Geophys. Res. 114, D08127. doi:10.1029/2008jd010844.
Robock, A., Vinnikov, K.Y., Srinivasan, G., Entin, J.K., Hollinger, S.E., Speranskaya, N.A., Liu, S., Namkhai, A., 2000. The global soil moisture data bank. Bull. Amer. Meteor. Soc. 81, 1281–1299.
Roujean, J.L., Leroy, M., Deschamps, P.Y., 1992. A bidirectional reflectance model of the Earth's surface for the correction of remote sensing data. J. Geophys. Res. 97 (20), 455–468.
Sassen, K., DeMott, P.J., Prospero, J.M., Poellot, M.R., 2003. Saharan dust storms and indirect aerosol effects on clouds: CRYSTAL-FACE results. Geophys. Res. Lett. 30.
Schepanski, K., Tegen, I., Todd, M.C., et al., 2009. Meteorological processes forcing Saharan dust emission inferred from MSG-SEVIRI observations of subdaily dust source activation and numerical models. J. Geophys. Res. 114, D10201.
Schlichting, H., 1936. Experimentelle untersuchungen zum rauhigkeitsproblem. Ingen.-Arch 7, 1–34.
Schulz, M., Balkanski, Y., Guelle, W., Dulac, F., 1998. Role of aerosol size distribution and source location in a three-dimensional simulation of a Saharan dust episode tested against satellite derived optical thickness. J. Geophys. Res. 103, 10579–10592.
Scipal, K., Drusch, M., Balsamo, G., de Rosnay, P., 2009. Assimilation of global ASCAT soil moisture observations in the ECMWF Numerical Weather Prediction Model. Geophys. Res. Abs. 11, EGU2009-12881.
Seino, N., Sasaki, H., Yamamoto, A., Mikami, M., 2005. Numerical simulation of mesoscale circulation in the Tarim Basin associated with dust events. J. Meteorol. Soc. Japan 83A, 205–218.
Sekiyama, T.T., Tanaka, T.Y., Shimizu, A., Miyoshi, T., 2010. Data assimilation of CALIPSO aerosol observations. Atmos. Chem. Phys. 10, 39–49.
Shao, Y., 2004. Simplification of a dust emission scheme and comparison with data. J. Geophys. Res. 109, D10202. doi:10.1029/2003JD004372.
Shao, Y., 2008. Physics and Modeling of Wind Erosion, 2nd ed. Springer Science, p. 452.
Shao, Y., Dong, C.H., 2006. A review on East Asian dust storm climate, modeling and monitoring. Glob. Planet. Change 52, 1–22.
Shao, Y., Leslie, L.M., 1997. Wind erosion prediction over the Australian continent. J. Geophys. Res. 102, 30091–30105.
Shao, Y.P., 2000. Physics and Modelling of Wind Erosion. Kluwer Academy, Dordrecht, Netherlands.
Shao, Y., Wang, J., 2003. A climatology of Northeast Asian dust events. Meteorologische Zeitschrift 12, 175–183.
Shao, Y., Yang, Y., 2008. A theory for drag partition over rough surfaces, J. Geophys. Res. 113, F02S05. doi:10.1029/2007JF000791.
Shao, Y., Raupach, M.R., Findlater, P.A., 1993. The effect of saltation bombardment on the entrainment of dust by wind. J. Geophys. Res. 98, 12719–12726.
Shao, Y., Raupach, M.R., Leys, J.F., 1996. A model for predicting aeolian sand drift and dust entrainment on scales from paddock to region. Aust. J. Soil Res. 34, 309–342.
Shao, Y., Yang, Y., Wang, J., Song, Z., Leslie, L. M., Dong, C., Zhang, Z., Lin, Z., Kanai, Y., Yabuki, S., Chun, Y., 2003. Northeast Asian dust storms: Real-time numerical prediction and validation. J. Geophys. Res. 108, D22, 4691. doi:10.1029/2003JD003667.
Shao, Y.P., Leys, J.F., McTainsh, G.H., Tews, K., 2007. Numerical simulation of the October 2002 dust event in Australia. J. Geophys. Res. 112, D08207. doi:10.1029/2006JD007767.
Shao, Y., Fink, A.H., Klose, M., 2010. Numerical simulation of a continental-scale Saharan dust event. J. Geophys. Res. 115, D13205. doi:10.1029/2009JD012678.
Shao, Y., Ishizuka, M., Mikami, M., Leys, J., 2011. Parameterization of size-resolved dust emission and validation with measurements, J. Geophys. Res.
Sherman, D.J., 1990. Evaluation of aeolian sand transport equations using intertidal-zone measurements, Saunton Sands, England. Sedimentology 37, 385–388.
Shi, P., Yan, P., Yuan, Y., Nearing, M.A., 2004. Wind erosion research in China: Past, present and future. Prog. Phys. Geograp. 28, 366–386.
Shinoda, M., Nandintsetseg, B., 2011. Moisture and vegetation memories in a cold, arid climate, Global Planetary Change (under review).
Shinoda, M., Ito, S., Nachinshonhor, G.U., Erdenetsetseg, D., 2007. Phenology of Mongolian grasslands and moisture conditions. J. Meteor. Soc. Japan 85, 359–367.
Shinoda, M., Kimura, R., Mikami, M., Tsubo, M., Nishihara, E., Ishizuka, M., Yamada, Y., Munkhtsetseg, E., Jugder, D., Kurosaki, Y., 2010a. Characteristics of Dust Emission on the Mongolian Steppe: The 2008 DUVEX Intensive Observational Period. SOLA 6, 9–12.
Shinoda, M., Nachinshonhor, G.U., Nemoto, M., 2010b. Impact of drought on vegetation dynamics of the Mongolian steppe: a field experiment. J. Arid Environ. 74, 63–69.
Siddoway, F.H., Chepil, W.S., Armbrust, D.V., 1965. Effect of Kind, Amount, and Placement of Residue on Wind Erosion Control. Trans. ASAE 8, 327–331.
Skidmore, E.L., Tatarko, J., 1990. Stochastic wind simulation for erosion modeling. Trans. ASAE 33, 1893–1899.
Sokolik, I.N., Winker, D.M., Bergametti, G., Gillette, D.A., Carmichael, G., Kaufman, Y.J., Gomes, L., Schuetz, L., Penner, J.E., 2001. Introduction to special section: Oustanding problems in quantifying the radiative impacts of mineral dust. J. Geophys. Res. 106, 18015–18027.
Sow, M., Alfaro, S.C., Rajot, J.L., Marticorena, B., 2009. Size resolved dust emission fluxes measured in Niger during 3 dust storms of the AMMA experiment. Atmos. Chem. Phys. 9, 3881–3891.
Stockton, P.H., Gillette, D.A., 1990. Field measurements of the sheltering effect of vegetation on erodible land surfaces. Land. Degrad. Rehabilit. 2, 77–86.
Stout, J.E., Zobeck, T.M., 1996. The Wolfforth Field Experiment: a wind erosion study. Soil. Sci. 161, 616–632.
Sugimoto, N., Uno, I., Nishikawa, M., Shimizu, A., Matsui, I., Dong, X., Chen, Y., Quan, H., 2003. Record Heavy Asian Dust in Beijing in 2002: Observations and Model Analysis of Recent Events, Geophys. Res. Letters 30, 12, 1640. doi:10.1029/2002GL016349.
Sugimoto, N., Matsui, I., Shimizu, A. et al., 2006. Network observations of Asian dust and air pollution aerosols using two-wavelength polarization lidars. 23rd International Laser Rader Conference, July 2006 Nara, Japan, 23ILRC, ISBN 4-9902916-0-3. pp. 851–854.
Sugita, M., Asanuma, J., Tsujimura, M., Mariko, S., Lu, M., Kimura, F., Azzaya, D., Adyasuren, Ts., 2007. An overview of the rangelands atmosphere–hydrosphere–biosphere interaction study experiment in northeastern Asia (RAISE). J. Hydrol. 333, 3–20.
Sutton, S.L.F., McKenna Neuman, C., 2008. Sediment entrainment to the lee of roughness elements: effects of vortical structures. J. Geophys. Res. 113, F02S09. doi:10.1029/2007JF000783.
Svensson, A., Biscaye, P.E., Grousset, F.E., 2000. Characterization of late glacial continental dust in the Greenland Ice Core Project ice core. J. Geophys. Res. 105 (D4), 4637–4656.
Tanaka, T.Y., Chiba, M., 2005. Global simulation of dust aerosol with a chemical transport model, MASINGAR. J. Met. Soc. Japan 83A, 255–278.
Tanaka, T.Y., Chiba, M., 2006. A numerical study of the contributions of dust source regions to the global dust budget. Global Planet Change 52, 88–104.
Tegen, I., Fung, I.Y., 1994. Modeling mineral dust in the atmosphere: sources, transport, and optical thickness. J. Geophys. Res. 99, 22897–22914.
Tegen, I., Fung, I., 1995. Contribution to the atmospheric mineral aerosol load from land surface modification. J. Geophys. Res. 100 (D9), 18707–18726.
Theurer, W., 1973. Dispersion of ground-level emissions in complex built-up areas. Ph.D. thesis. University of Karlsruhe.
Todd, M.C., Karam, D.B., Cavazos, C., Bouet, C., Heinold, B., Baldasano, J.M., Cautenet, G., Koren, I., Perez, C., Solmon, F., Tegen, I., Tulet, P., Washington, R., Zakey, A., 2008. Quantifying uncertainty in estimates of mineral dust flux: An intercomparison of model performance over the Bodélé Depression, northern Chad. J. Geophys. Res. 113, D24107. doi:10.1029/2008JD010476.
UNEP, 1997. World Atlas of Desertification, second ed. Arnold, London, p. 182.
Uno, K., Harada, S., Satake, Hara, Y., Wang, Z., 2005. Meteorological characteristics and dust distribution of the Tarim Basin simulated by the nesting RAMS/CFORS dust model. J. Meteorol. Soc. Japan 83A, 219–239.
Uno, I., Eguchi, K., Yumimoto, K., Takemura, T., Shimizu, A., Uematsu, M., Liu, Z., Wang, Z., Hara, Y., Sugimoto, N., 2009. Asian dust transported one full circuit around the globe. Nature Geoscience, Published Online: 20 July 2009. doi:10.1038/NGEO583.
USDA-NRCS, 1999. Soil taxonomy: a basic system of soil classification for making and interpreting soil surveys. In: USDA-NRCS Agriculture Handbook (second ed.), U.S. Government Printing Office, Washington, DC, p. 870.
Van Oost, K., Quine, T.A., Govers, G., De Gryze, S., Six, J., Harden, J.W., Ritchie, J.C., McCarty, G.W., Heckrath, G., Kosmas, C., Giraldez, J.V., Marquez da Silva, J.R., Merckx, R., 2007. The impact of agricultural soil erosion on the global carbon cycle. Science 318, 626–629.
Vogel, B., Hoose, C., Vogel, H., Kottmeier, C., 2006. A Model of dust transport applied to the Dead Sea Area. Meteorologische Zeitschrift 6, 611–624.

Please cite this article in press as: Shinoda, M., et al. Temperate grasslands as a dust source: Knowledge, uncertainties, and challenges. Aeolian Research (2011), doi:10.1016/j.aeolia.2011.07.001

Walker, J.P., Houser, P.R., 2001. A methodology for initializing soil moisture in a global climate model: assimilation of near–surface soil moisture observations. J. Geophys. Res. 106, 11761–11774.

Wang, X., Oenema, O., Hoogmoed, W.B., Perdok, U.D., Cai, D., 2006. Dust storm erosion and its impact on soil carbon and nitrogen losses in northern China. Catena 66, 221–227.

Washington, R., Todd, M.C., 2005. Atmospheric controls on mineral dust emission from the Bodélé Depression, Chad: the role of the low level jet. Geophys. Res. Lett. 32. doi:10.1029/2005GL023597.

Wasson, R.J., Nanninga, P.M., 1986. Estimating wind transport of sand on vegetated surfaces. Earth Surf. Process. Landforms 11, 505–514.

Westphal, L., Toon, O.B., Carlson, T.N., 1988. A case study of mobilization and transport of Saharan dust. J. Atmos. Sci. 45, 2145–2175.

Wiegand, T., Snyman, H.A., Kellner, K., 2004. Do grasslands have a memory: modeling phytomass production of a semiarid South African grassland. Ecosystems 7, 243–258.

Wiegand, T., Wiegand, K., Pütz, S., 2008a. Grassland models. In: Jørgensen, S.E. (Ed.), Ecological Models Encyclopedia of Ecology. Elsevier, Oxford, pp. 1754–1765.

Wiegand, K., Saltz, D., Ward, D., Levin, S.A., 2008b. The role of size inequality in self-thinning: a pattern-oriented simulation model for arid savannas. Ecol. Model. 210, 431–445.

Wolfe, S.A., Nickling, W.G., 1996. Shear stress partitioning in sparsely vegetated desert canopies. Earth. Surf. Proc. Land. 21, 607–619.

Wooding, R., Bradley, E.F., Marshall, J.K., 1973. Drag due to regular roughness elements of varying geometry.. Bound-Layer Meteorol 5, 285–308.

Woodruff, N.P., Siddoway, F.H., 1965. A wind erosion equation. Soil. Sci. Soc. Am. Proc. 29 (5), 602–608.

Wyatt, V.E., Nickling, W.G., 1997. Drag and shear stress partitioning in sparce desert Creosote communities. Canadian J. Earth Sci. 34, 1486–1498.

Yang, G., Xiao, H., Tuo, W., 2001. Black windstorm in northwest China: a case study of the strong sand-dust storm on May 5th 1993. Dust and Sandstorms from the World's Drylands. Report of United Nations Global Alarm, 49–73.

Yang, Y., Shao, Y., 2005. Drag partition and its Implication to Dust Emission. Water. Air. Soil. Poll: Focus. 5, 251–259.

Yumimoto, K., Uno, I., Sugimoto, N., Shimizu, A., Liu, Z., Winker, D.M., 2008. Adjoint inversion modeling of Asian dust emission using lidar observations. Atmos. Chem. Phys. 8, 2869–2884.

Zender, C.S., Bian, H., Newman, D., 2003. Mineral dust entrainment and deposition (DEAD) model: description and 1990s dust climatology. J. Geophys. Res. 108(D14), 4416. doi:10.1029/2002JD002775.

Zhu, Z., Shu, L., Zheng, W., 1980. Deserts of China. Science Press, Beijing, 107p (in Chinese).

Zobeck, T.M., Fryrear, D.W., 1986. Chemical and physical characteristics of windblown sediment II. Chemical characteristics and nutrient discharge. Trans. Amer. Soc. Agric. Eng. 29, 1032–1036.

Zobeck, T.M., 1991. Soil properties affecting wind erosion. J. Soil Water Conserv. 46, 112–118.

Zou, X.K., Zhai, P.M., 2004. Relationship between vegetation coverage and spring dust storms over northern China. J. Geophys. Res. 109, D03104. doi:10.1029/2003JD003913.

Please cite this article in press as: Shinoda, M., et al. Temperate grasslands as a dust source: Knowledge, uncertainties, and challenges. Aeolian Research (2011), doi:10.1016/j.aeolia.2011.07.001